Igneous evolution of a complex laccolith-caldera, the Solitario, Trans-Pecos Texas: Implications for calderas and subjacent plutons

Christopher D. Henry* *Nevada Bureau of Mines and Geology, University of Nevada, Reno, Nevada 89557*
Michael J. Kunk *U.S. Geological Survey, Reston, Virginia 20192*
William R. Muehlberger *Department of Geological Sciences, University of Texas, Austin, Texas 78712*
W. C. McIntosh *Department of Geoscience, New Mexico Institute of Mining and Technology, Socorro, New Mexico 87801*

ABSTRACT

The Solitario is a large, combination laccolith and caldera (herein termed "laccocaldera"), with a 16-km-diameter dome over which developed a 6 × 2 km caldera. This laccocaldera underwent a complex sequence of predoming sill, laccolith, and dike intrusion and concurrent volcanism; doming with emplacement of a main laccolith; ash-flow eruption and caldera collapse; intracaldera sedimentation and volcanism; and late intrusion. Detailed geologic mapping and $^{40}Ar/^{39}Ar$ dating reveal that the Solitario evolved over an interval of approximately 1 m.y. in three distinct pulses at 36.0, 35.4, and 35.0 Ma. The size, duration, and episodicity of Solitario magmatism are more typical of large ash-flow calderas than of most previously described laccoliths.

Small volumes of magma intruded as abundant rhyolitic to trachytic sills and small laccoliths and extruded as lavas and tuffs during the first pulse at 36.0 Ma. Emplacement of the main laccolith, doming, ash-flow eruption, and caldera collapse occurred at 35.4 Ma during the most voluminous pulse. A complex sequence of debris-flow and debris-avalanche deposits, megabreccia, trachyte lava, and minor ash-flow tuff subsequently filled the caldera. The final magmatic pulse at 35.0 Ma consisted of several small laccoliths or stocks and numerous dikes in caldera fill and along the ring fracture. Solitario rocks appear to be part of a broadly cogenetic, metaluminous suite.

Peralkaline rhyolite lava domes were emplaced north and west of the Solitario at approximately 35.4 Ma, contemporaneous with laccolith emplacement and the main pulse in the Solitario. The spatial and temporal relation along with sparse geochemical data suggest that the peralkaline rhyolites are crustal melts related to the magmatic-thermal flux represented by the main pulse of Solitario magmatism.

Current models of laccolith emplacement and evolution suggest a continuum from initial sill emplacement through growth of the main laccolith. Although the Solitario laccocaldera followed this sequence of events, our field and $^{40}Ar/^{39}Ar$ data demonstrate that it developed through repeated, episodic magma injections, separated by 0.4 to 0.6 m.y. intervals of little or no activity. This evolution requires a deep, long-lived magma source, well below the main laccolith.

Laccoliths are commonly thought to be small, shallow features that are not representative of major, silicic magmatic systems such as calderas and batholiths. In contrast, we suggest that magma chambers beneath many ash-flow calderas are tabular, floored intrusions, including laccoliths. Evidence for this conclusion includes the following: (1) many large plutons are recognized to be laccoliths or at least tabular, (2) the Solitario and several larger calderas are known to have developed over laccoliths, and (3) magma chambers beneath calderas, which are as much as 80 km in diameter, cannot be as deep as they are wide or some would extend into the upper mantle. The Solitario formed during a tectonically neutral period following Laramide deformation and preceding Basin and Range extension. Therefore, space for the main laccolith was made by uplift of its roof and possibly subsidence of the floor, not by concurrent faulting. Laccolith-type injection is probably a common way that space is made for magma bodies of appreciable areal extent in the upper crust.

INTRODUCTION

Laccoliths and calderas are, respectively, two of the most common and interesting intrusive and extrusive expressions of magmatism. Otherwise, they would seem to have little in common. Laccoliths and other concordant intrusions have been intensely studied since the nineteenth century (e.g., Gilbert, 1887; Corry, 1988; Jackson and Pollard, 1988; Roman-Berdiel et al., 1995). However, both the earliest and many recent studies emphasized small, shallowly emplaced examples such that the prevalent view may be that all laccoliths are small, shallow, short-lived, and not representative of voluminous terrestrial magma systems such as calderas and batholiths (Mudge, 1968; Corry, 1988; Hanson and Glazner, 1995; Roman-Berdiel et al., 1995). For example, the *Glossary of Geology* (Bates and Jackson, 1987, p. 364) specifies that laccoliths are "generally . . . less than five miles in diameter, and from a few feet to several hundred feet in thickness."

Calderas have also been intensely studied and are known to be among the largest and longest-lived volcanic systems, commonly undergoing episodic activity over 1 m.y. or more (Smith and Bailey, 1968; Lipman, 1984; Cas and Wright, 1987). The association of calderas with underlying plutons or batholiths is well established (Lipman, 1984). Considerable field and modeling research has addressed the style of caldera collapse (Druitt and Sparks, 1984; Lipman, 1984; Walker, 1984; Komuro, 1987; Scandone, 1990; Marti et al., 1994; Branney, 1995). However, the shape of the underlying magma body has been little discussed, in part because at most only the top of the former magma chamber is exposed in most calderas. The mechanism by which space is made for the caldera magma chamber is an unresolved problem (Lipman et al., 1984), and a problem for large intrusions in general. Although mushroom-shaped or

*E-mail: chenry@nbmg.unr.edu

GSA Bulletin; August 1997; v. 109; no. 8; p. 1036–1054; 12 figures, 1 table.

flat magma chambers have been inferred by some (Smith, 1979; Scandone, 1990), probably most geologists picture spherical or deep cylindrical bodies beneath calderas, not laccoliths.

It has been recognized that many plutons are tabular and include laccoliths (Hamilton and Myers, 1967; Bergantz, 1991; Brown, 1994; Vigneresse, 1995). Marsh (1989) stated that the nearer to the surface a magma chamber reaches, the more sheetlike it becomes, and sheetlike bodies are generally much more voluminous than tall bodies. Modeling by Clemens and Mawer (1992) indicates that granitic magmas should rise along fractures and generate laccolithic or thin, floored plutons of all sizes at any depth. Despite these studies, recent attempts to solve the space problem—i.e., the way in which granite plutons make space in the upper or middle crust—have focused on the role of contemporaneous faulting (e.g., Hutton, 1988; Petford et al., 1993; Hanson and Glazner, 1995), although the importance of laccoliths is beginning to be emphasized (Morgan and Law, 1996; Petford, 1996). Similarly, the possibility that caldera magma chambers are tabular has not received wide recognition, although laccolith-caldera systems have been described (Hildebrand, 1984; Henry and Price, 1989).

In contrast, we suggest that the magma chambers of many calderas (and plutons in general) were laccoliths or otherwise thin, floored bodies. This view is based on detailed mapping and $^{40}Ar/^{39}Ar$ dating of the Solitario (Henry and Muehlberger, 1996; Henry and Kunk, 1996), a laccolith-caldera complex (herein termed "laccocaldera") in Trans-Pecos Texas (Figs. 1 and 2), and on published descriptions of numerous tabular plutons and a few other laccocalderas.

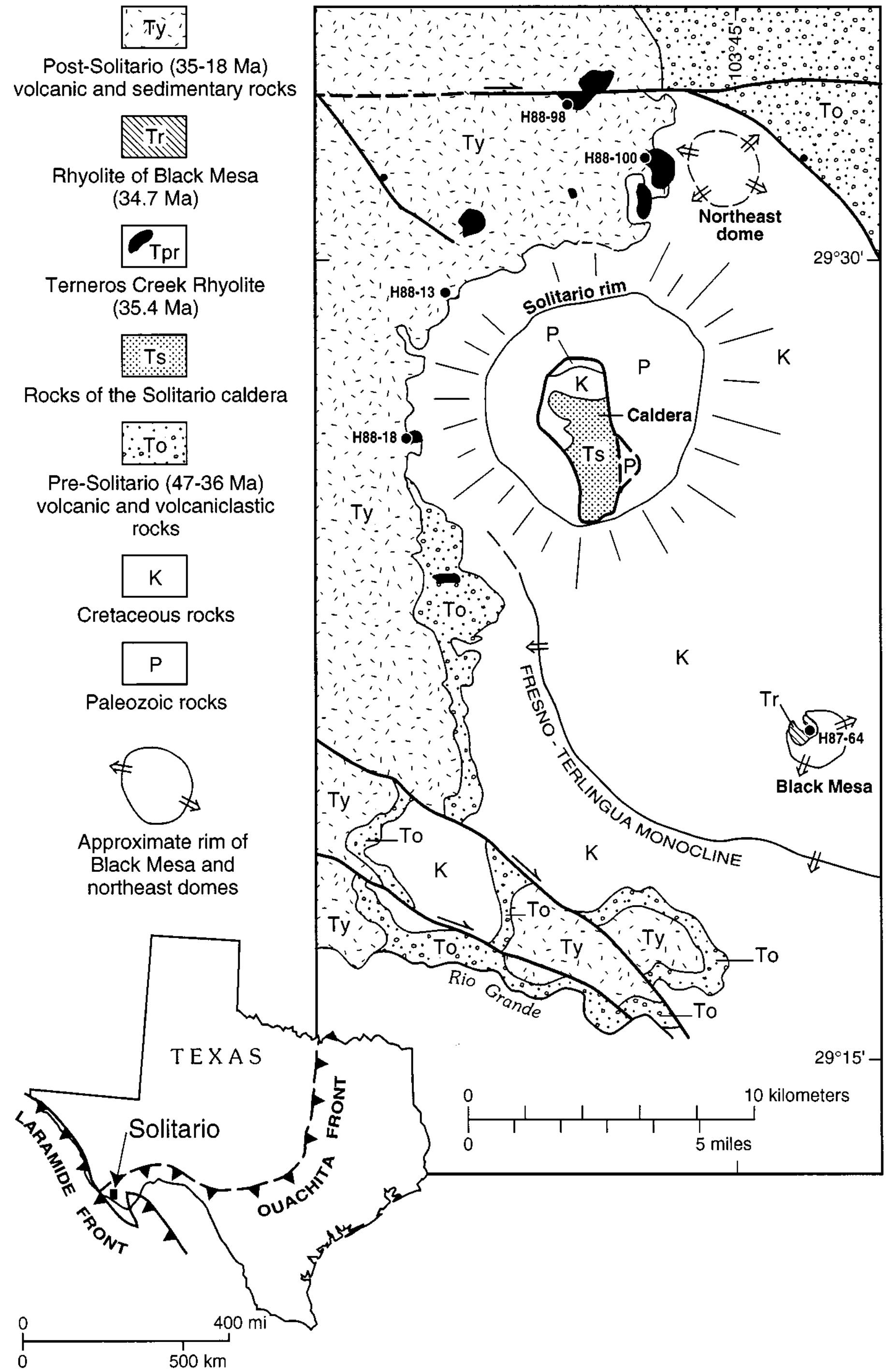

Figure 1. Location and generalized geology of the Solitario, Trans-Pecos Texas. The Terneros Creek Rhyolite consists of peralkaline rhyolite lava domes that erupted at approximately 35.4 Ma, contemporaneously with the main pulse of activity, laccolithic doming, ash-flow eruption, and caldera collapse in the Solitario.

What is a Laccolith?

Laccoliths were recognized by Gilbert (1877), who specified both an intrusive shape and mechanism of emplacement. Laccoliths are floored intrusions over which host strata are domed. They form when magma rises vertically in a dike or other narrow conduit, spreads between horizontal strata as a sill, and then lifts the overlying strata so that they bend concordantly over the intrusion (see also Daly, 1933; Corry, 1988; Jackson and Pollard, 1988). Although attempts have been made to distinguish laccoliths and sills on the basis of thickness/diameter ratios, most summaries have emphasized that there is complete gradation between the two (Gilbert, 1877; Daly, 1933; Corry, 1988). A meaningful distinction may be that strata are distinctly arched over a laccolith and are only negligibly so over a sill. We think a multikilometer-thick concordant intrusion should be called a laccolith, regardless of diameter and of curvature or flatness of the roof, because such a thick body must make space by lifting its roof and/or depressing its floor. In this report, we use "laccolith" where we are reasonably certain of intrusive shape and where cited authors use the term; where less certain, we refer to "floored, tabular intrusions."

Geologic Setting of the Solitario

The Solitario developed between 36 and 35 Ma, during the 38 to 32 Ma main phase of magmatism in Trans-Pecos Texas (Henry and

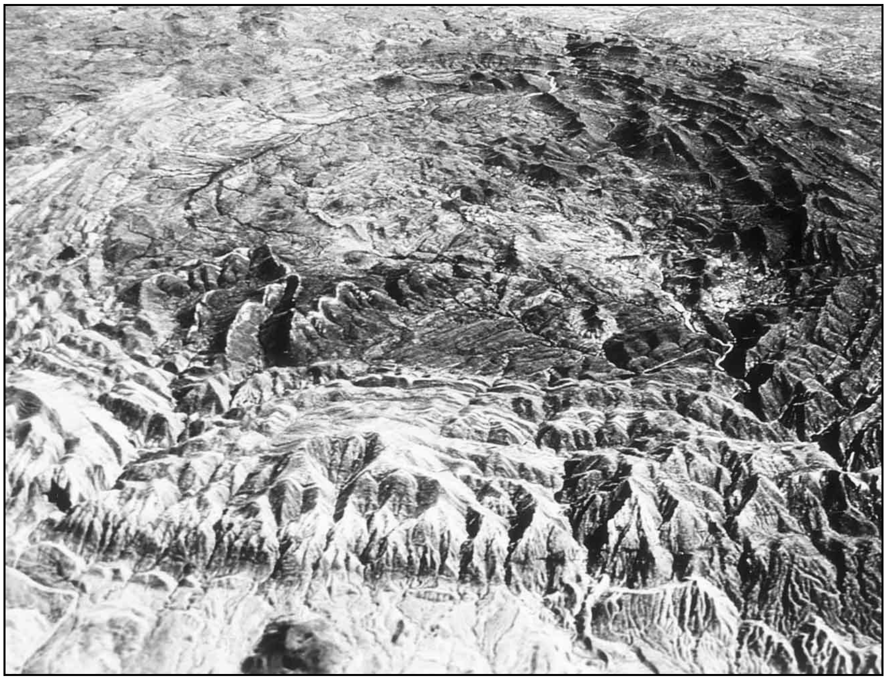

Figure 2. Oblique aerial view of the Solitario, looking northeastward across the dome. Cretaceous sedimentary rocks dip steeply and radially outward around the dome. These overlie folded and faulted Paleozoic rocks in the interior. The light-colored area in the center and right center is a 6 × 2 km caldera formed by eruption of ash-flow tuff from the underlying laccolith. Ash-flow tuff and debris deposits filling the caldera are relatively nonresistant to erosion, so the caldera is topographically low. Photograph courtesy of Mesa Operating Co., Inc.

McDowell, 1986). Numerous calderas, ranging up to 30 km in diameter, formed from the eruption of widespread, voluminous ash-flow tuffs during this time (Henry and Price, 1984). The Solitario formed in the southern part of the province, near the eastern edge of the early Tertiary, Laramide fold belt and above the late Paleozoic, Ouachita-Marathon fold belt (Fig. 1).

Highly folded and thrust-faulted Paleozoic rocks of the Ouachita-Marathon fold belt, which crop out in the core of the Solitario dome, are the oldest exposed rocks (Figs. 1 and 3). These rocks were deposited in deep water southeast of what was then the margin of the North American continent and thrust northwestward over relatively undeformed Paleozoic rocks that were deposited in shallow water on the craton. Cretaceous marine sedimentary rocks, which were largely flat-lying before Solitario doming, unconformably overlie the folded Paleozoic rocks. The only significant, nearby Laramide fold is the Fresno-Terlingua monocline (Erdlac, 1990), which strikes into the southwestern rim of the Solitario (Fig. 1).

The Cretaceous rocks are overlain by a thin interval of upper Eocene tuffaceous sedimentary rocks (Fig. 3). Several rhyolite lava domes, collectively called the Terneros Creek Rhyolite, erupted contemporaneously with Solitario doming in an arc north and west of the dome (Fig. 1). These predoming volcanic rocks are overlain by the thick Solitario Conglomerate, which resulted from erosion of the Solitario and is preserved north and west of the dome. A variety of younger volcanic rocks overlie and interfinger with the conglomerate (Henry et al., 1997).

Geometry of the Solitario Dome and Caldera

The Solitario dome forms a nearly perfect circle about 16 km in diameter (Figs. 2 and 3; Herrin, 1957; Corry et al., 1990; Henry and Muehlberger, 1996). A resistant rim of radially outward dipping, Lower Cretaceous limestone surrounds a basin of generally less resistant Paleozoic rocks. Because the Cretaceous rocks were flat lying before doming, except along the southwest margin where the dome is superposed on the Laramide Fresno-Terlingua monocline, they provide excellent structural markers.

At the broadest scale, the Cretaceous rocks curve continuously through 360° of strike around the rim and dip radially outward, mostly between 30° and 40°. Part of the rim, particularly the southwestern part, consists of distinct, 1–1.5-km-long panels of nearly constant strike. The southwestern rim is steeper, and the southeastern rim more gentle, than other parts. Dips along the southwestern rim commonly reach 55°, which we interpret to indicate superposition upon the southwest-dipping Fresno-Terlingua monocline (Fig. 1). Dips along the southeastern rim are at most 28°. The southeastern rim is superposed upon the structurally high Terlingua uplift, the upthrown side of the monocline (Erdlac, 1990).

The dome appears to be doubly hinged, similar to host rocks of laccoliths of the Henry Mountains, Utah (Jackson and Pollard, 1988). An outer, concave-upward hinge is best shown in the southwest, where dip decreases outward through the upper part of the Cretaceous section into pre-Solitario Tertiary rocks (Fig. 3). Even 8 km from the center of the dome, the pre-Solitario Tertiary rocks dip 4° to 6° outward. Because Cretaceous rocks are eroded from the interior of the dome, we used apparent tilts of minor folds and other structures in the Paleozoic rocks to estimate the degree of tilt (Henry and Muehlberger, 1996). These data suggest that tilt decreased inward across a series of modest hinges. Nevertheless, steep dips were maintained well into the interior of the dome; probably only the central 2 to 3 km of the dome were flat. The claims of Corry et al. (1990) that the dome flattens to nearly horizontal along a hinge that coincides closely with the inner edge of Cretaceous outcrop and that the entire interior of the dome was nearly flat are not supported by field data (Henry et al., 1994).

From the known and inferred geometry, we estimate the maximum amplitude of the dome to be approximately 2.5 km (Henry and Muehlberger, 1996). The volume of the underlying laccolith is approximately 90 km^3, assuming a laccolith radius of 6 to 7 km. Note that the laccolith is smaller than the dome because tilting commonly extends beyond the edge of the laccolith (Jackson and Pollard, 1988). In addition, we estimate that the main laccolith was emplaced at an original depth of about 4 km, probably along the sole thrust of the Ouachita-Marathon fold belt (Fig. 3). This estimate is based in part upon the relationship between radius of a laccolith and effective mechanical thickness of overburden (Pollard and Johnson, 1973; Jackson and Pollard, 1988; Roman-Berdiel et al., 1995). Physical and other modeling demonstrates that laccolith emplacement requires an extensive, planar, subhorizontal, soft layer (Dixon and Simpson, 1987; Clemens and Mawer, 1992; Roman-Berdiel et al., 1995). The sole thrust, which lay at a depth of 3 to 4 km, is the shallowest such layer in the otherwise highly deformed Paleozoic rocks.

Although the main laccolith is not exposed, the geometry of the Solitario indicates that it is a laccolith rather than a stock (Lonsdale, 1940; Corry et al., 1990; Henry and Muehlberger, 1996). The Solitario is geometrically similar to domes for which a laccolithic origin is well established (Gilbert, 1877; Corry, 1988; Jackson and Pollard, 1988). The steep monoclinal flexures and hinges on the flanks (Fig. 3), gentle outward decrease in dip, and stacking of innumerable sills over the dome are typical of laccoliths (Gilbert, 1877; Jackson and Pollard, 1988; Corry, 1988). Corry et al. (1990) interpret gravity and aeromagnetic data to indicate a floored intrusion. Furthermore, many nearby intrusions in Trans-Pecos Texas are demonstrably laccoliths and have locally exposed floors (Lonsdale, 1940; Maxwell et al., 1967; Henry and Price, 1989).

The Solitario caldera is 6×2 km and elongate north-northwest (Figs. 1 and 3). Subsidence occurred along a distinct ring fracture that can be traced continuously around the caldera. Collapse was highly asymmetric, greater in the south than in the north. Displacement on the northern boundary is no more than 1 km; precollapse rocks crop out within the caldera and dip steeply southward. The southern boundary had 2 to 2.5 km of displacement, which, combined with the probable thickness of the laccolith magma body, suggests that the southern end of the caldera block could have bottomed on the base of the laccolith.

$^{40}Ar/^{39}Ar$ Methodology

$^{40}Ar/^{39}Ar$ ages were obtained on 13 samples that span the time of activity recognized from field relations in the Solitario, as well as on some adjacent rocks (Table 1; Fig. 4). All analyses are of high-purity separates of alkali feldspar phenocrysts. Samples were crushed, ground, sieved to 60 to 80 mesh, concentrated with standard magnetic and density techniques, and leached with dilute HF. Final cleanup to >99% purity involved additional magnetic and density separation, HF leaching, and, rarely, handpicking.

Ages were determined in the U.S. Geological Survey laboratory in Reston, Virginia. Analytical methods were discussed in detail by McIntosh et al. (1990), and complete analytical data are available from Henry upon request. Samples were irradiated in the U.S. Geological Survey TRIGA reactor (Dalrymple et al., 1981) for 20 hr. Fish Canyon sanidine (FCT-3, 27.79 Ma, relative to an age of 519.4 Ma on MMhb-1; Alexander et al., 1978; Dalrymple et al., 1981; Kunk et al., 1985) was used as a neutron fluence monitor. We heated approximately 250 to 500 mg aliquots at 650 to 750 °C to melt sample capsules and to drive off low-temperature gas fractions, which are likely to have a significant atmospheric Ar component. Analyses of this step in many samples have shown that it contains <1% of the total reactor-produced ^{39}Ar. Samples were then heated incrementally in six to eight 10-min steps at between 950 and 1450 °C (Fig. 4).

Spectra for all samples developed plateaus using the definition of Fleck et al. (1977). Uncertainties in ages are 0.12 or 0.13 m.y. (1σ). All data reduction was done using an updated version of the program ArAr* (Haugerud and Kunk, 1988).

IGNEOUS EVOLUTION OF THE SOLITARIO

Magmatism in the Solitario occurred between 36 and 35 Ma in at least three distinct pulses that are distinguished by field relations, petrographic characteristics, and $^{40}Ar/^{39}Ar$ ages (Fig. 5). Numerous sills and a small laccolith intruded Cretaceous and Paleozoic rocks and were accompanied by minor lavas during the earliest pulse at 36.0 Ma. During the second, main pulse at 35.4 Ma, the main laccolith and radial dikes were emplaced, the dome formed, and ash-flow eruption and caldera collapse occurred. Numerous dikes and small laccoliths intruded during the third pulse at about 35.0 Ma.

Solitario igneous activity was mostly silicic to intermediate; only one basalt is present that may be related to Solitario magmatism. Solitario rocks are also moderately alkalic, but less so than many other igneous suites of Trans-Pecos Texas, some of which are peralkaline (Price et al., 1987). This difference helps to distinguish Solitario rocks petrographically; they contain biotite phenocrysts (Fig. 6), whereas the more alkalic rocks lack biotite and may contain sodic amphibole or pyroxene. For example, peralkaline rhyolite lava domes of the Terneros Creek Rhyolite, which erupted around the Solitario contemporaneously with the main pulse, contain arfvedsonite.

First Pulse: Rim Sills, Related Lavas, and Syenite

Numerous silicic to intermediate intrusions and related volcanic rocks were emplaced before doming during the earliest igneous activity of the Solitario. These form two groups: (1) the "rim sills," consisting of mostly rhyolitic sills in Cretaceous and Paleozoic rocks, and (2) syenitic and rhyolitic intrusions near the future caldera.

Rim Sills and Related Volcanic Rocks (T1). Abundant rhyolitic to trachytic sills, dikes, and one laccolith were emplaced into Lower Cretaceous and Paleozoic rocks before doming. Petrographically similar rhyolitic lava domes and flows that are preserved in situ within the caldera, as megabreccia blocks in the caldera, and northwest of the Solitario are probably extrusive equivalents.

All previous workers recognized what has been called the "rim sill" and implied that it was a single intrusion into the base of the Cretaceous section in the rim (Powers, 1921; Lonsdale, 1940; Corry et al., 1990). In fact, the rim sill consists of multiple intrusions that we group into three map units based on petrographic type: aphyric rhyolite (Tir1), porphyritic rhyolite (Tir2), and porphyritic trachyte (Tit1) (Figs. 6 and 7). Aphyric and porphyritic rhyolite are about equally abundant; porphyritic trachyte forms only a few intrusions in the northeast rim and in Paleozoic rocks north of the caldera.

These rocks were emplaced mostly as sills and mostly into the lowermost Cretaceous section or into Paleozoic rocks. Sills are present nearly continuously around the rim, except for about 80° of the southeast rim, and are thickest and most abundant in the northern and western rim, where cumulative thickness reaches about 400 m (Fig. 3). The presence of several megabreccia blocks in the southeastern part of the caldera (Fig. 3) consisting of Cretaceous rocks with sills indicates that sills once extended nearly to the present southeastern rim. Sills are also abundant in the highly folded and thrust-faulted Paleozoic rocks, particularly shale-rich parts northeast of the caldera, despite the structural complexity of the hosts. Sills are most common in limbs of folds where attitudes of the host rock remain constant for moderate distances, but some sills wrap around fold axes. Several sills intrude along thrust faults (Fig. 7). Although we conclude later herein that most doming of the Solitario occurred during the second pulse of activity, emplacement of as much as 400 m of sills at depths of about 1 km probably induced some doming.

Observed feeders to sills in the rim are uncommon. However, a few sills in steeply dipping Paleozoic rocks can be traced continuously into sills in Cretaceous rocks. These steeply dipping sills may have served the same purpose as dikes that fed sills elsewhere (Hyndman and Alt, 1987; Corry, 1990).

The number of individual sills is large but unknown. In any one section of the rim as many as six sills can be distinguished on the basis of rock type, stratigraphic position, and separation by continuous screens of Cretaceous rocks a few meters to about 15 m thick (Figs. 3 and 7). In several places, two bodies of aphyric rhyolite are separated by thin (1 to 2 m thick) screens of Cretaceous rock that terminate along strike. However, minor topographic or color boundaries that continue in the same stratigraphic position suggest separate sills.

A laccolith of porphyritic rhyolite, about 1.5 km in diameter and 600 to 800 m thick, intruded Cretaceous rocks in the northern rim. Cretaceous rocks above the laccolith are domed, whereas rocks below the laccolith bend downward. This relation is consistent with observations that sills and laccoliths deform both overlying and underlying beds (Pollard and Johnson, 1973).

Both aphyric and porphyritic rhyolite magmas appear to have fed lava domes or flows over

A

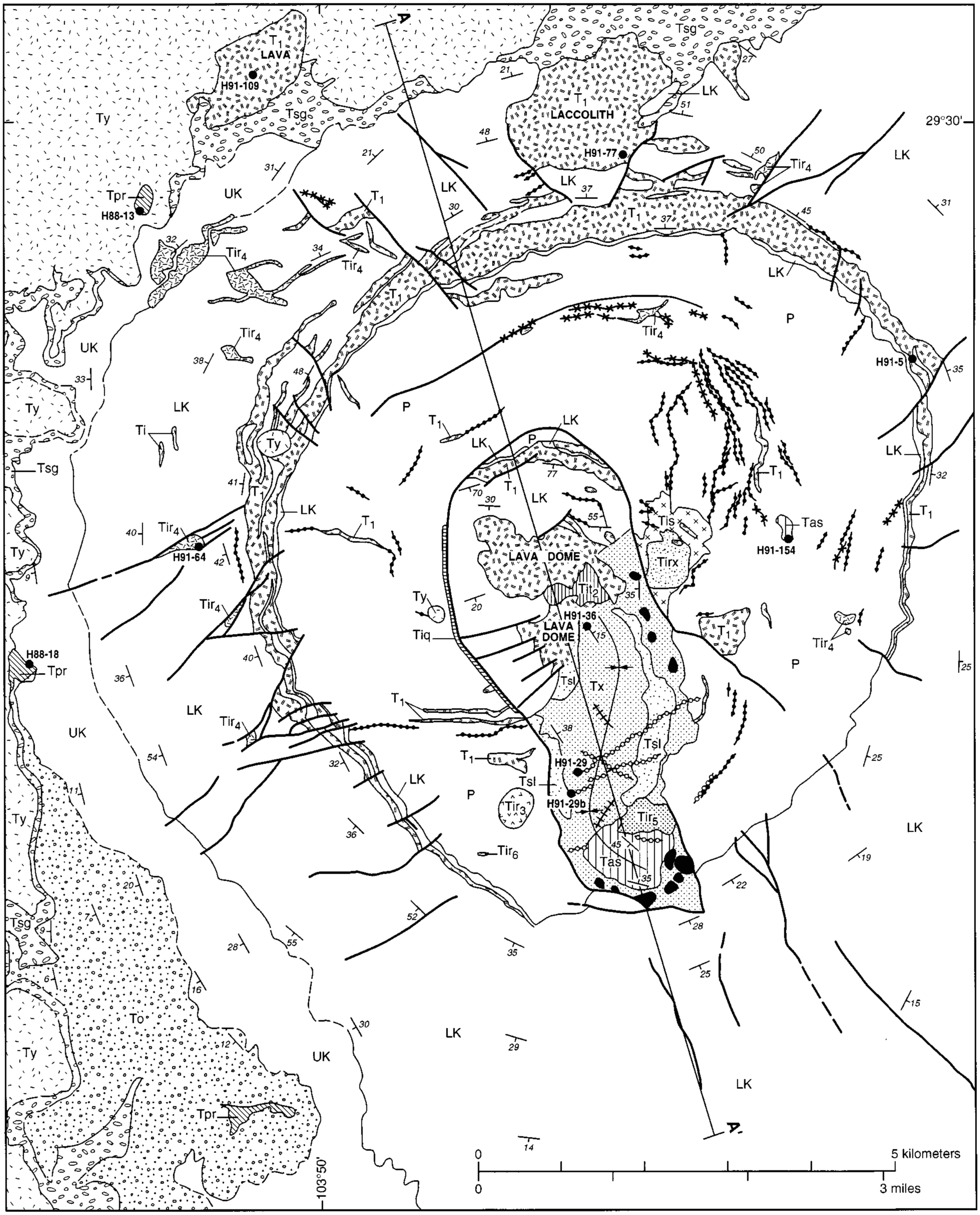

Figure 3. (A) Simplified geologic map and (B) cross section of the Solitario (from Henry and Muehlberger, 1996) showing igneous rocks that formed during the three distinct pulses of activity. Numerous sills, dikes, and small laccoliths and related volcanic rocks were emplaced during the first pulse at 36.0 Ma (T1); they cannot be completely subdivided at the scale of this figure (but see Fig. 7). During the second and most voluminous pulse at 35.4 Ma, radial dikes were intruded, the ash-flow tuff erupted, and the caldera collapsed. Doming and emplacement of the unexposed, main laccolith also occurred at this time. Numerous small intrusions were emplaced in and around the caldera during the final pulse at 35.0 Ma.

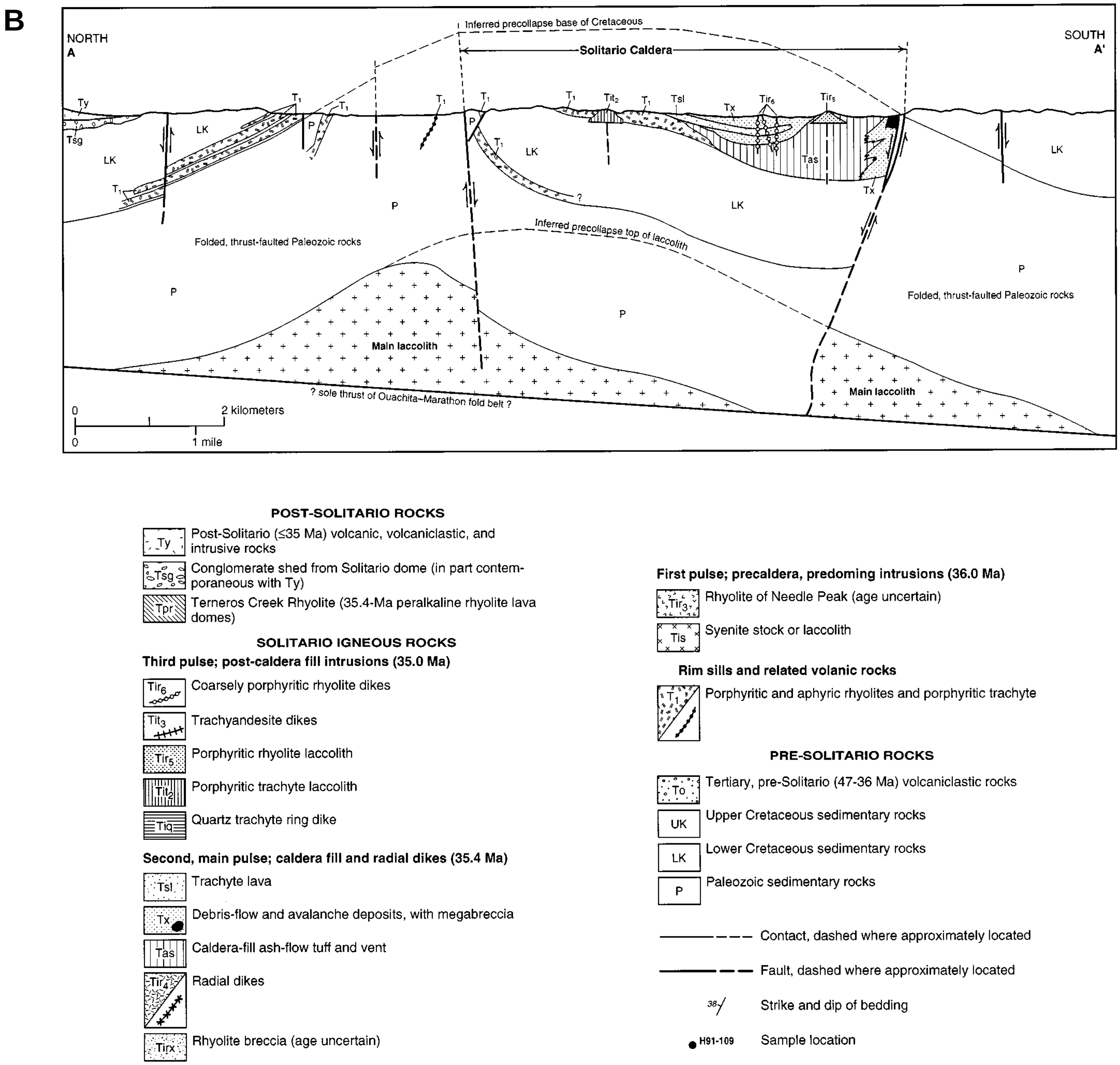

the top of what was to become the Solitario. Lava domes and related pyroclastic deposits of aphyric rhyolite that crop out within the northern and central part of the caldera (Fig. 3) are probable extrusive equivalents of the aphyric sills. The domes rest upon uppermost Cretaceous rocks and are overlain by caldera-filling debris deposits (Tx) or trachyte lava (Tvt). These relations indicate that the domes were emplaced before caldera collapse.

Porphyritic rhyolites are represented by the lava flow northwest of the dome, by a megabreccia block within the caldera, and by abundant clasts in the Solitario Conglomerate (Tsg; Fig. 3). Correlation is based on petrographic similarity, field constraints, and, for the flow, indistinguishable $^{40}Ar/^{39}Ar$ ages (Table 1). The megabreccia block, which is about 200 m long, consists of two flows of porphyritic rhyolite. Presumably, this block was part of a sequence of lavas that overlay the Solitario before doming. No flows are preserved in situ, but their prevalence as clasts in Solitario Conglomerate west of the dome indicates that they must have been abundant.

Early emplacement of these sills, before major doming and caldera collapse of the Solitario, is indicated by field relations and by $^{40}Ar/^{39}Ar$ ages (Table 1; Fig. 5). Sills are cut by faults related to doming and by quartz-phyric rhyolites (Tir4) that intrude along the faults. Sills in Cretaceous rocks in the downdropped caldera block and in Paleozoic rocks outside the caldera are truncated by the caldera boundary fault (Fig. 3). Several megabreccia blocks within the caldera consist of Cretaceous limestone with sills. Locally, aphyric rhyolite appears to crosscut porphyritic rhyolite,

TABLE 1. $^{40}Ar/^{39}Ar$ DATA ON ALKALI FELDSPAR FROM IGNEOUS ROCKS OF THE SOLITARIO AND VICINITY

Unit	Sample	Lat (°N)	Long (°W)	Plateau age (Ma)	^{39}Ar (%)
Rhyolite of Black Mesa (Tr)					
	H87-64	29 21.3	103 43.6	34.71 ± 0.12	56.0
Terneros Creek Rhyolite (Tpr)					
	H88-13	29°29.5	103°51.4	35.46 ± 0.12	85.4
	H88-18	29°26.7	103°51.8	35.26 ± 0.12	60.2
	H88-98	29°33.0	103°48.5	35.58 ± 0.12	100
	H88-100	29°31.5	103°46.0	35.38 ± 0.12	83.8
Solitario igneous rocks					
Third pulse					
Coarsely porphyritic rhyolite dikes (Tir6)					
	H91-29	29°25.9	103°48.1	34.92 ± 0.12	94.7
	H91-29b	29°25.8	103°47.9	34.99 ± 0.12	62.2
Second, main pulse					
Ash-flow tuff and vent of the Solitario (Tas)					
	H91-36	29°26.8	103°48.2	35.29 ± 0.12	100
	H91-154	29°27.4	103°46.7	35.40 ± 0.12	83.0
Quartz-phyric (radial) dikes (Tir4)					
	H91-64	29°27.3	103°50.9	35.51 ± 0.12	82.6
First pulse					
Rhyolite lava equivalent to rim sills					
	H91-109	29°30.3	103°50.6	35.95 ± 0.13	71.4
Rim sills (Tir2)					
	H91-5	29°28.5	103°45.8	36.02 ± 0.13	82.1
	H91-77	29°29.8	103°47.8	36.03 ± 0.13	64.0

Note: $\lambda_\beta = 4.963 \times 10^{-10}$ yr^{-1}; $\lambda_{\varepsilon + \varepsilon'} = 0.581 \times 10^{-10}$ yr^{-1}; $^{40}K/K = 1.167 \times 10^{-4}$.

and vice versa. Three $^{40}Ar/^{39}Ar$ ages determined on porphyritic rhyolite, including a sill in the northeastern rim, the northern laccolith adjacent, and the lava in the northwest, range from 36.03 ± 0.13 to 35.95 ± 0.13 Ma. All are indistinguishable within the limits of analytical uncertainty. We infer that the aphyric rhyolite and porphyritic trachyte intrusions were emplaced at the same time on the basis of field relations.

The volume of this early magmatism is difficult to estimate because of disruption by caldera collapse and extensive erosion. However, a minimum volume would be about 22 km^3 if sills average 200 m thick across a 12-km-diameter circle. Related volcanic rocks might add another 10 km^3.

Porphyritic Syenite (Tis). A complex intrusion of porphyritic syenite, about 1.5 × 1 km, is exposed along and is truncated by the eastern margin of the caldera (Fig. 3). Outcrop and subsurface data from mineral exploration drill holes (Corry et al., 1990) suggest that the syenite rose as a stock that spread laterally along a southeast-dipping thrust fault. Field relations indicate the syenite was contemporaneous with the rim sill rhyolites. The syenite is cut by both aphyric and porphyritic rhyolite dikes (Fig. 3), but several sills of aphyric rhyolite strike into but do not cut the syenite along its northeastern margin. This area is poorly exposed, and it is possible that the sills simply terminated at the contact and are not cut by the syenite. The syenite is cut by the eastern boundary fault of the caldera, so definitely predated caldera collapse.

Rhyolite of Needle Peak (Tir3). The rhyolite of Needle Peak consists of a small plug and a thick, discontinuous dike of sparsely porphyritic rhyolite that are separated from intruded Paleozoic rocks by a thick breccia of the same rhyolite and host rock. The contact between breccia and Paleozoic rock dips steeply inward, suggesting explosive eruption through an upward-widening vent. Time of emplacement of the rhyolite of Needle Peak is unknown. The surrounding breccia suggests shallow emplacement, which would require that the dome be already uplifted and deeply eroded. However, if the caldera had existed at the time of intrusion, the rhyolite likely would have been emplaced along the caldera fault or extruded into the caldera.

Main Pulse: Radial Dikes, Ash-Flow Eruption, Laccolith Emplacement, and Formation of the Solitario Dome

The second and most voluminous pulse of activity occurred at about 35.4 Ma and included emplacement of the main laccolith; doming; intrusion of quartz-phyric, radial dikes (Tir4); eruption of the ash-flow tuff of the Solitario (Tas); and possibly emplacement of rhyolite breccia (Tirx). $^{40}Ar/^{39}Ar$ ages ranging from 35.51 ± 0.12 Ma to 35.29 ± 0.12 Ma indicate that this second pulse occurred long after emplacement of the early sills at 36.0 Ma.

Rhyolite Breccia (Tirx). An intrusion of rhyolite breccia 500 to 700 m across contains angular to moderately rounded clasts of aphyric and porphyritic rhyolite and Paleozoic rocks in a felsic, pumiceous groundmass. The breccia intrudes porphyritic syenite just east of the caldera (Fig. 3), is cut by quartz-phyric rhyolite dikes (Tir4), and is cut by the eastern boundary fault of the caldera. These field relations indicate that it was emplaced before doming or caldera collapse, possibly early during the main pulse. It may be a vent for the main ash-flow tuff that was terminated by caldera collapse or for a minor, earlier eruption.

Quartz-Phyric Rhyolite Dikes (Tir4). Petrographically distinct, finely porphyritic rhyolite (Tir4; Fig. 6) forms (1) generally radial dikes and some sills in the Cretaceous rim, (2) dikes, sills, and irregular intrusions in Paleozoic rocks, and (3) dikes in porphyritic syenite (Tis) and rhyolite breccia (Tirx) east of the caldera. These rhyolites, which are restricted to the northern part of the Solitario, are the second-most abundant of the exposed intrusive types.

The dated dike in the western rim (Fig. 3) is the best example of the radial dikes. It thickens toward the center of the dome from no more than 5 m on the west to about 200 m on the east. This and several other quartz-phyric rhyolites entrain xenoliths of Paleozoic and Cretaceous rocks. Notably, the western dike contains abundant clasts of Cretaceous limestone up to 15 cm in diameter along its margin. The dike is strongly flow banded parallel to the margin, which, along with the abundant lithics, gives the appearance of welded tuff. Cretaceous rocks adjacent to the dike are brecciated.

Quartz-phyric rhyolites that cut Paleozoic rocks in the northern part of the basin form a crudely concentric band that follows a fault that was previously interpreted to be a Paleozoic thrust (Corry et al., 1990). However, the fault is steeply dipping, and we have reinterpreted it as a circumferential, doming fault (Henry and Muehlberger, 1996).

We interpret the quartz-phyric dikes to have intruded along radial and concentric fractures during doming and to be offshoots from the main laccolith. The increase in thickness of the dated dike may reflect increased inward separation of the Cretaceous rocks during doming. The quartz-phyric rhyolites may represent incipient or initial eruption of the laccolith magma chamber that eventually led to ash-flow eruption and caldera collapse. The dated dike gives an $^{40}Ar/^{39}Ar$ age on alkali feldspar of 35.51 ± 0.12 Ma (Table 1; Fig. 5).

Ash-Flow Tuff and Vents (Tas). Coarsely porphyritic, densely welded, devitrified, quartz-trachyte ash-flow tuff (Fig. 8) crops out in the southern part of the caldera and commonly forms clasts in overlying debris deposits throughout the rest of the caldera (Fig. 3). A definite vent is present about 1.7 km east of the caldera, and several probable but poorly preserved vents lie along the northern caldera boundary fault.

The exposed tuff is about 150 m thick, rests upon coarse debris deposits (Tx), and is overlain by other debris deposits. Variations in abundances of lithic fragments, which consist of Paleozoic rocks, possible Cretaceous limestone, and various igneous rocks, suggest that the tuff consists of several flows that compose a single cooling unit. A basal lithic accumulation layer a few meters thick contains 50% to 70% clasts up to 1.5 m in diameter. Lithic abundance decreases abruptly to 10% to 20% above the base. A 1–1.5-m-thick layer about 30 m above the base contains 50% lithics up to 110 cm in diameter, mostly of a porphyritic igneous rock that is mineralogically similar to the host tuff and may represent relatively nonvesiculated magma lumps. This layer probably separates different ash flows. The tuff also contains clasts of itself that must have been derived from early erupted tuff, possibly deposited on the rim of the caldera. The progression in lithic and pumice abundance and size suggests changes in the intensity of eruption, possibly related to changes in vent diameter (Wilson et al., 1980).

Additional tuff may underlie exposed tuff. The base of caldera fill is nowhere exposed in the southern part of the caldera, and the presence of clasts of welded tuff within, and of debris deposits beneath, tuff outcrops indicate that some tuff eruption and collapse preceded deposition of exposed tuff. On the basis of the amount of collapse in the southern part of the caldera, intracaldera tuff could be nearly 1 km thick there (Fig. 3).

The tuff dips northward beneath debris deposits and does not reappear in the northern part of the caldera. However, debris deposits in that area contain clasts of densely welded ash-flow tuff up to 3 m in diameter. The clasts indicate that tuff cropped out near the northern margin of the caldera, either within the caldera or on its rim. In addition, low-level aeromagnetic data (Fig. 10) are consistent with a wedge of ash-flow tuff that thins progressively to the north. A distinct positive magnetic anomaly coincides with ash-flow tuff outcrops in the southern part of the caldera. Ash-flow tuff probably ponded preferentially in the southern part of the caldera because that part subsided first and most (Henry and Muehlberger, 1996).

The definite vent 1.7 km east of the caldera is an elongate stock about 300 by 150 m that cuts Paleozoic rocks. The rock is vesicular, vertically flow banded, and contains 10% to 30% angular clasts of Paleozoic rocks up to 13 cm in diameter (Fig. 9). Although most of the body is intensely altered, less-altered rock along the southern margin contains a distinctive phenocryst assemblage indistinguishable from that in the ash-flow tuff and unlike that in any other exposed igneous rock of the Solitario. We interpret this body to be a vent, frozen above the level of vesiculation but below the level of explosive magma fragmentation.

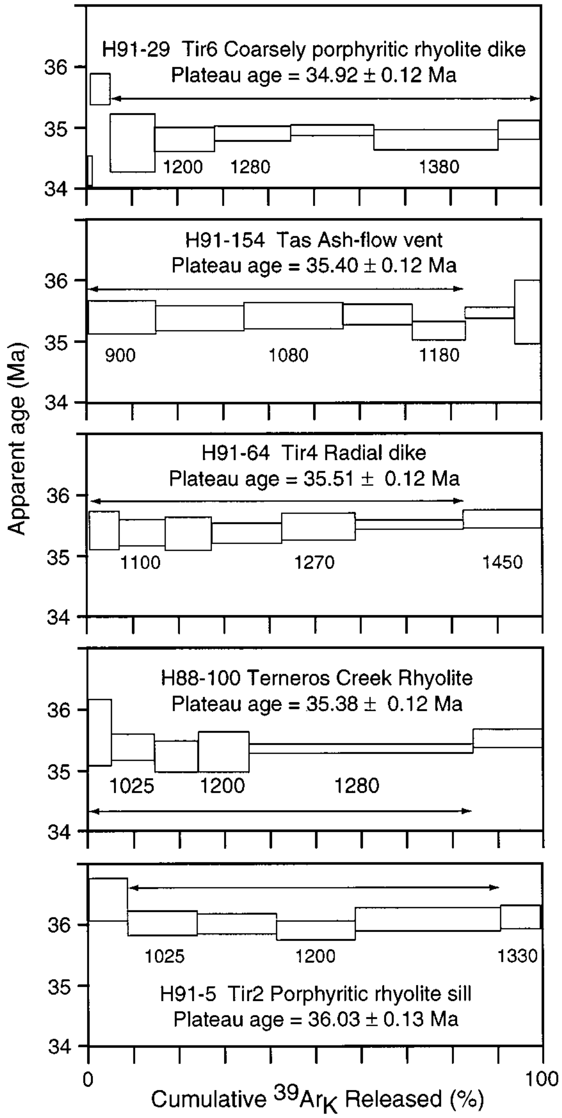

Figure 4. Representative $^{40}Ar/^{39}Ar$ age spectra for igneous rocks of the Solitario and Terneros Creek Rhyolite (see Table 1). Plateau age is defined using criteria of Fleck et al. (1977). Arrows show increments used in plateau. Numbers show selected extraction temperatures (°C).

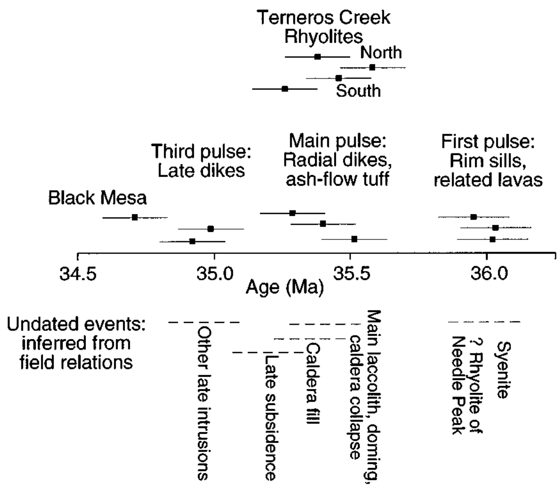

Figure 5. $^{40}Ar/^{39}Ar$ ages with 1σ error bars for dated rocks of the Solitario and Terneros Creek Rhyolite. Also shown are inferred ages for undated rocks based on field relations. Activity in the Solitario occurred in at least three brief episodes separated by long periods of repose.

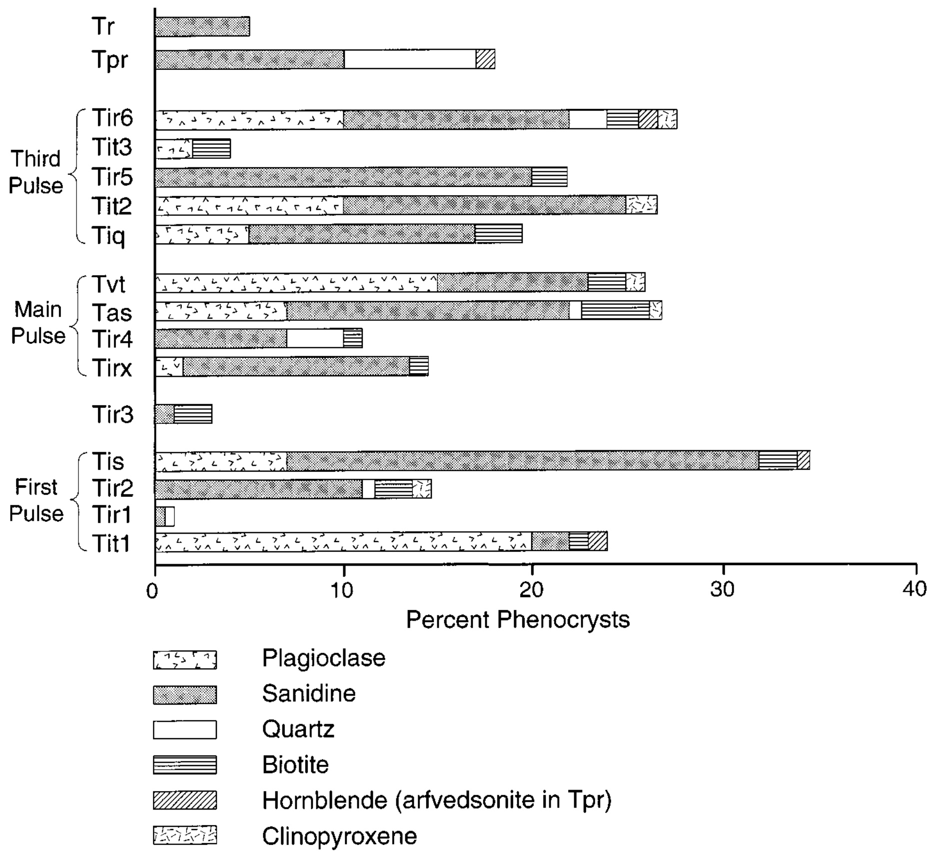

Figure 6. Phenocryst abundances of igneous rocks of the Solitario. The different groups are distinguished by phenocryst abundance and size and by field relations and $^{40}Ar/^{39}Ar$ age.

Probable vents along the northern caldera boundary consist of a series of discontinuous outcrops of coarsely clastic tuff. These bodies are covered by talus except in arroyo cuts but may be more continuous along the boundary. Although highly altered, the rocks have recognizable tuffaceous matrices, locally with coarse phenocrysts of alkali feldspar and biotite, and are petrographically similar to the ash-flow tuff. We interpret these bodies to be ash-flow vents that were disrupted during caldera collapse.

The volume of ash-flow tuff is unknown but is probably between 2 and 20 km^3. The smaller value is an estimate for intracaldera tuff from its outcrop area and reasonable subsurface extrapolation. The larger volume is based on the area and amount of subsidence of the asymmetric caldera. This estimate assumes that all collapse resulted from evacuation of the underlying magma chamber. Both estimates are limited by uncertainties in subsurface geometry, a ubiquitous problem for estimating tuff volumes. Obviously, only a small part of the tuff ponded within the caldera. Correlative outflow deposits, other than what was deposited on the immediate caldera rim and reworked into debris deposits, have not been recognized despite exposure of the appropriate stratigraphic interval immediately west of the caldera.

$^{40}Ar/^{39}Ar$ ages on alkali feldspar from the tuff and from the major vent are 35.29 ± 0.12 and 35.40 ± 0.12 Ma, respectively (Table 1; Fig. 5). These ages overlap within analytical uncertainty, and certainly the tuff and vent should have indistinguishable ages. Ponding of tuff within the caldera indicates that eruption and caldera collapse were contemporaneous, as is true for almost all calderas (Lipman, 1984).

Caldera-fill Debris Deposits and Lava (Tx and Tsl). A thick sequence of megabreccia, debris-flow and debris-avalanche deposits, and lava fill the caldera. These are well exposed along both sides of a roughly north-striking syncline resulting from late subsidence of the caldera (Fig. 3), and a semiregular stratigraphy can be followed around much of the caldera. The lowest exposed deposits, which mostly underlie the caldera-forming ash-flow tuff and probably overlie buried tuff at the southern end of the caldera (Fig. 3), are extremely coarse, unstratified, laterally discontinuous breccias. They contain common Paleozoic clasts and megabreccia blocks up to 200 m across near the southern and eastern caldera walls (Fig. 3). Most blocks are Cretaceous rocks, several with early sills, but one consists of two lava flows of porphyritic rhyolite equivalent to the early porphyritic sills.

A middle sequence is coarse but distinctly less so than the underlying rocks, includes some well-bedded, laterally continuous deposits, has few megabreccia blocks, and generally lacks Paleozoic clasts. Layering is defined by abrupt changes in clast type or in maximum and average clast sizes with diffuse boundaries between layers. A porphyritic trachyte lava (Tvt) is interbedded with these deposits (Fig. 3). The highest deposits range from coarse and massive to relatively fine and well bedded, are distinctly continuous, lack any megabreccia, and include some massive, tuffaceous deposits that may be nonwelded ash-flow tuff.

The interbedding of ash-flow tuff, breccia, and debris deposits and general upward fining are characteristic of caldera-fill sequences (Lipman, 1976, 1984). These deposits indicate that caldera collapse occurred contemporaneously with ash-flow eruption and that the caldera was deepest immediately following eruption and collapse. Collapse created, nearly instantaneously, a large, deep, closed basin bounded by a nearly vertical scarp that may have been more than 1 km high in the southern part of the caldera. Continued failure of the caldera walls generated landslides and debris-avalanches that accumulated within the caldera, slowly filling it and reducing relief. Continuity of the trachyte lava and presence of fluvial deposits indicate that the caldera basin eventually became relatively flat.

Late subsidence that generated the north-striking syncline may have begun during deposition of the stratigraphically highest debris deposits, which dip less steeply than do lower deposits. Subsidence distinctly postdated initial ash-flow eruption and caldera collapse and so must represent a distinct event, possibly related to eruption of the late, small-volume tuffs.

Solitario Laccolith. The main laccolith of the Solitario is not exposed and, by our estimate, lies at a present depth of approximately 1.5 km (Henry and Muehlberger, 1996). Nevertheless, its characteristics can be inferred from comparison with the ash-flow tuff, from geophysical data, and from comparison with other major, caldera-related intrusions in Trans-Pecos Texas.

The ash-flow tuff is the eruptive equivalent of an underlying magma chamber, which is most likely the laccolith. A large pumice fragment, which is generally considered the best indication of magma composition (Walker, 1972), contains approximately 65% SiO_2 and high total alkalies, probably reflecting the abundant feldspar phenocrysts (Henry, 1996). Therefore, the main laccolith likely consists of quartz monzonite, the coarse-grained equivalent of tuff of that composition, composed of alkali feldspar, plagioclase, biotite, quartz, and clinopyroxene, all of which are phenocrysts in the tuff. This composition and mineralogy are similar to those of exposed resurgent intrusions of several calderas in Trans-Pecos Texas, particularly quartz monzonites in the Chinati Mountains and Infiernito calderas (Fig. 11; Cepeda and Henry, 1983; Henry et al., 1992).

Regional aeromagnetic data (Fig. 11) support the interpretation that the Solitario laccolith is compositionally like the resurgent intrusions. All calderas in Trans-Pecos Texas, as well as the Solitario, are expressed as positive magnetic anomalies (Fig. 11) that reflect the exposed or underlying, solidified magma body. Most notable are anomalies associated with the exposed resurgent intrusions of the Chinati Mountains and Infiernito calderas (Cepeda and Henry, 1983; Henry et al., 1992). The lower relief of the magnetic anomaly associated with the Solitario is consistent with the laccolith being covered by at least 1.5 km of sedimentary rock.

The low-level aeromagnetic map also illustrates both the magnetic signature of the buried laccolith and the influence of the caldera (Fig. 10). The map shows a positive anomaly outside and approximately outlining the caldera. The caldera is a magnetic low, except at the south end where a positive anomaly overlies exposed ash-flow tuff, the eruptive product of the laccolith. These features are consistent with a magnetic high above the remaining thick part of the laccolith outside the caldera and a relative low within the caldera where the underlying laccolith must be thinner by the amount of caldera collapse. The surrounding magnetic high drops off outward as the laccolith thins toward its margin. The steep negative anomaly immediately north of the ash-flow tuff coincides with a late porphyritic rhyolite intrusion (Tir5; Fig. 3), which may have been emplaced during a period of reversed polarity. Corry et al. (1990) interpreted the magnetic data to indicate buried mafic intrusions related to the mafic-intermediate volcano to the west in the Bofecillos Mountains (Fig. 11). However, only one such intrusion, a 200-m-wide trachyandesite laccolith, is present in the Solitario, and it has negligible expression in the magnetic map (Figs. 3 and 10).

Timing and Duration of the Main Pulse. We interpret laccolith emplacement, doming, radial-dike intrusion, ash-flow eruption, and caldera collapse and filling to be penecontemporaneous events at about 35.4 Ma (Table 1; Fig. 5). Although the $^{40}Ar/^{39}Ar$ ages of the dike, ash-flow vent, and ash-flow tuff match likely relative ages, they are analytically indistinguishable. Certainly the ash-flow tuff and its vent should have formed within a few days of each other. The analytical data allow intrusion of the radial dikes to have preceded ash-flow eruption by a significant interval. However, the dikes probably intruded during initial growth of the laccolith because the radial and concentric fractures along which the dikes intrude likely formed at that time. Ash-flow eruption may have begun when these same dome-related fractures connected the laccolith magma chamber to the surface. Doming and extensional fracturing over shallow magma chambers are effective in initiating eruption (Lipman, 1984). Ash-flow eruption and caldera collapse certainly terminated growth of the dome.

All these events probably occurred in a short time, probably much less than 10 000 yr. Even a magma chamber the size of the main laccolith would cool and solidify rapidly. An infinite sheet (sill) 2.5 km thick, the inferred thickness of the laccolith (Henry and Muehlberger, 1996), would solidify in less than 10 000 yr from conduction alone (Cathles, 1981). A laccolith that also lost heat by convection (hydrothermal circulation) would cool still more rapidly.

Filling of the caldera was probably also rapid. Trachyte lava (Tvt) overlies the ash-flow tuff separated by only a modest thickness of fill (Fig. 3), so the lava probably erupted soon after collapse. Both filling and late subsidence of caldera fill ended before 35.0 Ma, when coarsely porphyritic rhyolite dikes of the third pulse were intruded.

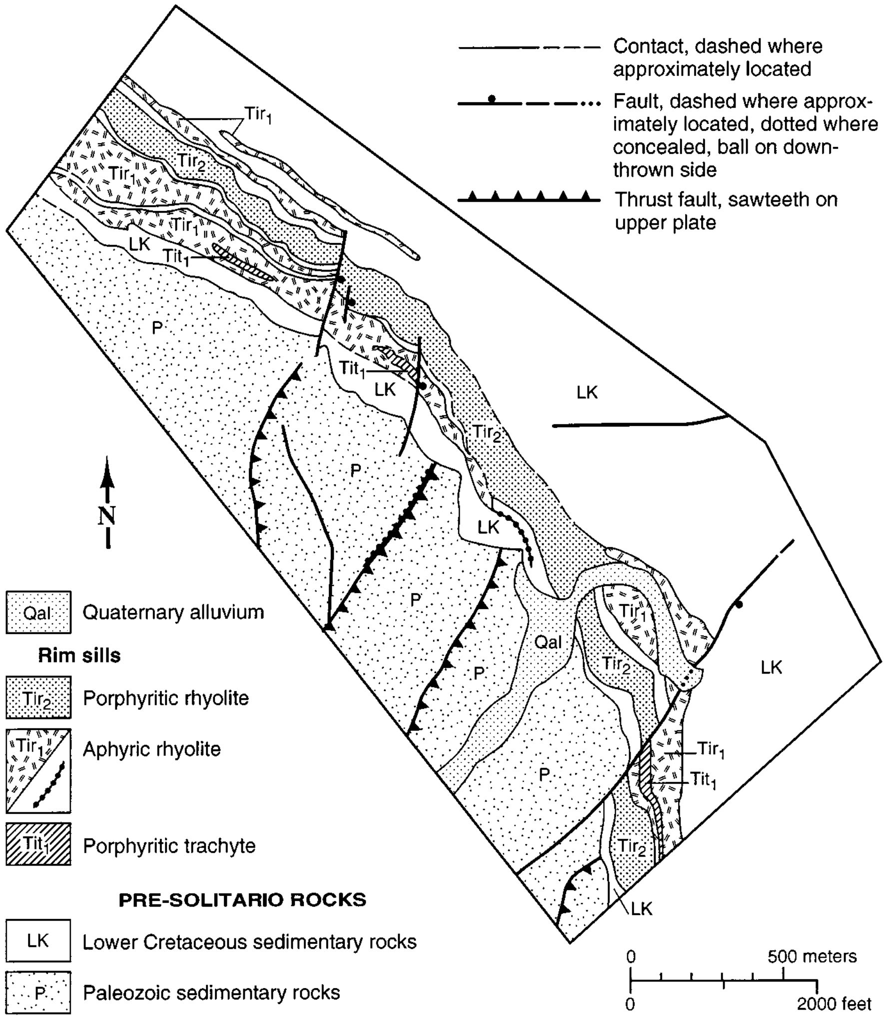

Figure 7. Geologic map of northeast rim of Solitario. At least six sills of the first pulse can be distinguished on the basis of rock type, stratigraphic position, and separation by continuous screens of Cretaceous rocks a few meters to about 15 m thick.

Third Pulse: Late Intrusions

The third pulse of magmatism in the Solitario consists of a series of dikes and small laccoliths emplaced in and around the caldera. $^{40}Ar/^{39}Ar$ ages of approximately 35.0 Ma are available for only two of the coarsely porphyritic rhyolite dikes (Tir6; Figs. 3 and 5), but field relations indicate that other intrusions are also late.

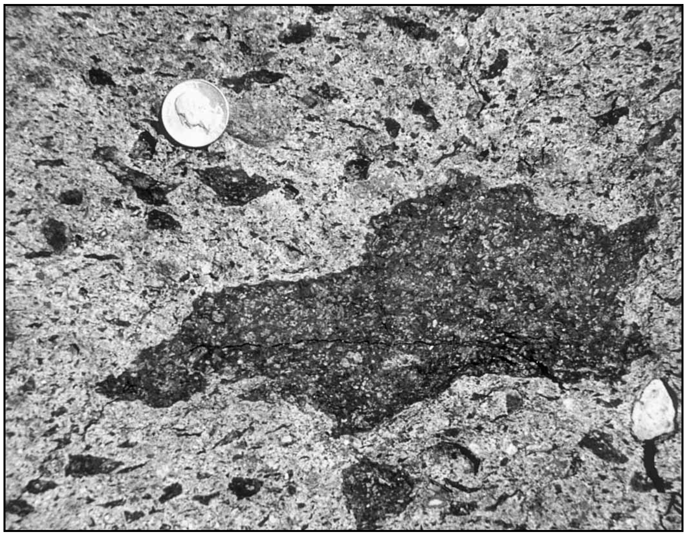

Figure 8. Densely welded ash-flow tuff of the Solitario, showing distinctive thick, dark pumice and lithic fragment of Paleozoic novaculite (lower right). $^{40}Ar/^{39}Ar$ age of tuff is 35.29 ± 0.12 Ma. Photograph is of a clast within caldera-fill debris deposits. Coin diameter is 2.5 cm.

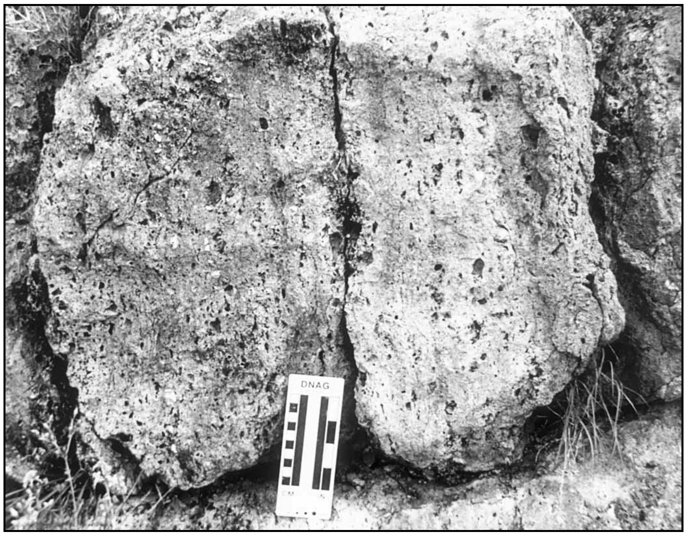

Figure 9. Outcrop of ash-flow vent. Rock is mostly vertically flow-banded, entrains numerous lithics up to 13 cm in diameter of Paleozoic rocks, and contains a phenocryst assemblage indistinguishable from that of the ash-flow tuff.

A group of mostly east-northeast–striking, vertical, coarsely porphyritic rhyolite dikes (Tir6) up to 8 m thick and 1.5 km long cuts caldera-fill debris deposits and ash-flow tuff in the southern part of the caldera. The dikes are distinguished by their complex phenocryst assemblage (Fig. 6), particularly the presence of alkali feldspars up to 1.7 cm long. The vertical attitude of the dikes across the syncline indicates that they were emplaced after late subsidence in the caldera. $^{40}Ar/^{39}Ar$ ages of 34.92 ± 0.12 and 34.99 ± 0.12 Ma on two dikes confirm a distinct, younger pulse of activity (Table 1; Fig. 5).

Other late intrusions include a 2-km-long quartz trachyte dike (Tiq) that was emplaced along the western ring fracture; an irregular, porphyritic trachyte laccolith(?) (Tit2) in the north-central part of the caldera; a porphyritic rhyolite laccolith(?) (Tir5) in the southern part of the caldera; and several sparsely porphyritic trachyte dikes (Tit3) (Fig. 3). All of these bodies either cut caldera fill or intrude along the ring fracture and must be younger than 35.4 Ma. Several also appear to have been emplaced after subsidence of the caldera. A biotite K-Ar age of 34.4 ± 0.8 Ma from the quartz trachyte dike (Tiq) is consistent with the $^{40}Ar/^{39}Ar$ ages (Henry and Kunk, 1996).

Several small pods of basalt intrude Cretaceous rocks along a fault, probably related to caldera collapse, in the northern part of the caldera. The time of emplacement and relationship to other igneous activity in the Solitario is unknown. However, its chemical composition in comparison to other basalts in the region indicates it is part of mid-Tertiary activity rather than part of younger, extension-related magmatism (James and Henry, 1991; Henry, 1996). Thus it could be a mafic part of the Solitario igneous system.

Terneros Creek Rhyolite; 35.4 Ma Magmatism Around the Solitario

At least eight peralkaline rhyolite lava domes (Terneros Creek Rhyolite; Fig. 1) erupted north and west of the Solitario about 35.4 Ma, contemporaneously with the main pulse of activity in the Solitario (Fig. 5). $^{40}Ar/^{39}Ar$ ages of four domes range from 35.26 ± 0.12 to 35.58 ± 0.12 Ma (Table 1; Fig. 5). This range exceeds 1σ uncertainty, thus the rhyolites may have erupted over a period of several hundred thousand years. However, field relations are not available to determine relative ages between the different domes, and only the youngest and oldest ages do not overlap at 1σ. Ages do not correlate with geographic position, so eruption did not migrate with time. Therefore, a mean age of 35.42 ± 0.13 Ma may be the best estimate of their age.

Regardless of the age span indicated by the data, the Terneros Creek Rhyolites erupted contemporaneously with the main pulse in the Solitario (Fig. 5). These rhyolites are present only near the Solitario. However, chemical and isotopic data indicate that the two groups are distinct and cannot have come from the same source, despite their contemporaneity and close spatial association. Chemical (Henry, 1996) and petrographic data (Fig. 6) show that the Terneros Creek Rhyolites are peralkaline, whereas all Solitario rocks are metaluminous. Intermediate and mafic rocks that could be parts of a differentiation suite occur in the Solitario but not with the peralkaline rhyolites. Pb isotopic data on two samples of Terneros Creek Rhyolite suggest that they were derived dominantly from the crust (James and Henry, 1993). The samples have low $^{206}Pb/^{204}Pb$ and $^{207}Pb/^{204}Pb$, similar to ratios in Precambrian basement and xenoliths of lower crustal rocks in Trans-Pecos Texas (James and Henry, 1993). Isotopic compositions of Solitario rocks have not been determined, but Pb and other geochemical data on similar silicic complexes in Texas indicate derivation from the mantle with variable crustal input (James and Henry, 1991, 1993).

We speculate that the Terneros Creek Rhyolites are lower crustal melts related to the large magma flux represented by the main pulse of activity in the Solitario. In contrast, we suggest that Solitario magmas are differentiates of mantle-derived basalt, likely with moderate crustal input. Similar interpretations of multiple magma sources related to crustal melting have been proposed for other laccolith systems (Nabelek et al., 1992).

Black Mesa Dome: 34.7 Ma Laccocaldera?

Black Mesa is another possible laccocaldera that developed 8 km southeast of the Solitario at 34.7 Ma (Table 1; Fig. 1). The Black Mesa dome has a width of 2.5 km and an amplitude of 180 m. Cretaceous limestone is nearly flat-lying over the top of the dome but dips between 20 and 30° on its flanks. The dome is circular and symmetrical except around the north and northwest flanks, where a large scallop is occupied by coarse, lithic tuff cut by a rhyolitic intrusion. A $^{40}Ar/^{39}Ar$ age on the rhyolite intrusion is 34.71 ± 0.12 Ma (Table 1). We infer that this is also the age of the laccolith, although the complexity of the Solitario suggests some caution, because the dome is so small that activity was likely to have been short-lived. The scallop on the northwest flank is either a caldera resulting from partial collapse of the dome or a crater where Cretaceous rocks were blown outward. The presence within tuff of blocks of Cretaceous rock that formerly covered the dome allows some collapse. By any interpretation, Black Mesa is a laccolithic dome that erupted pyroclastic material in an explosive event that removed part of its flank.

DISCUSSION

Episodic Versus Continuous Development of the Solitario

Evolution of the Solitario could involve either additional episodes or more continuous activity. Many intrusions are not dated, including ones we assign to each episode. However, most intrusions reasonably fit into one of the recognized pulses on the basis of field relations, intrusive setting, petrographic characteristics, or consideration of their likely origins. For example, intrusion of the radial dikes could have preceded emplacement of the main laccolith by as much as several hundred thousand years, on the basis of our $^{40}Ar/^{39}Ar$ ages (Fig. 5). This would require a separate injection of magma from a deeper source, because no shallow magma chamber would remain molten for that duration. Intrusion of the radial dikes as offshoots of, and contemporaneous with, the main laccolith seems more reasonable.

Regardless of the number of episodes or continuity of activity, the 1 m.y. duration of activity in the Solitario requires repeated injection of magma from a source deeper than the main laccolith. The same estimates on duration of the main pulse apply to the entire history. A magma body the size of the main laccolith could not remain as a magma source for even 100 000 yr.

The Solitario would seem to be unusual both as a laccolith and as a caldera. However, we suggest that in fact it is more representative of both, on the basis of the geology of the Solitario and published descriptions of other calderas, laccoliths, and plutons. This point is elaborated herein below.

Comparison with Other Laccoliths and Plutons

In comparing the Solitario to other laccoliths, a distinction needs to be made between the small, shallow laccoliths that have long been recognized and described in the literature (Gilbert, 1877; Johnson and Pollard, 1973; Hyndman and Alt, 1987; Corry, 1988; Jackson and Pollard, 1988) and larger, deeper laccoliths that are increasingly being recognized (see below). The Solitario is larger than these "traditional" laccoliths and has undergone a much more complex and episodic evolution. The vast majority of laccoliths in a recent compilation are less than 10 km across and 1 km thick (Corry, 1988). Comparison of size is slightly hampered because it is not always apparent whether the width of the intrusion or of the dome is cited. As shown by Jackson and Pollard (1988), the dome is significantly wider than the underlying intrusion. Using either criteria, the Solitario, with a dome diameter of at least 16 km and a probable intrusion diameter of 12 to 14 km, is large.

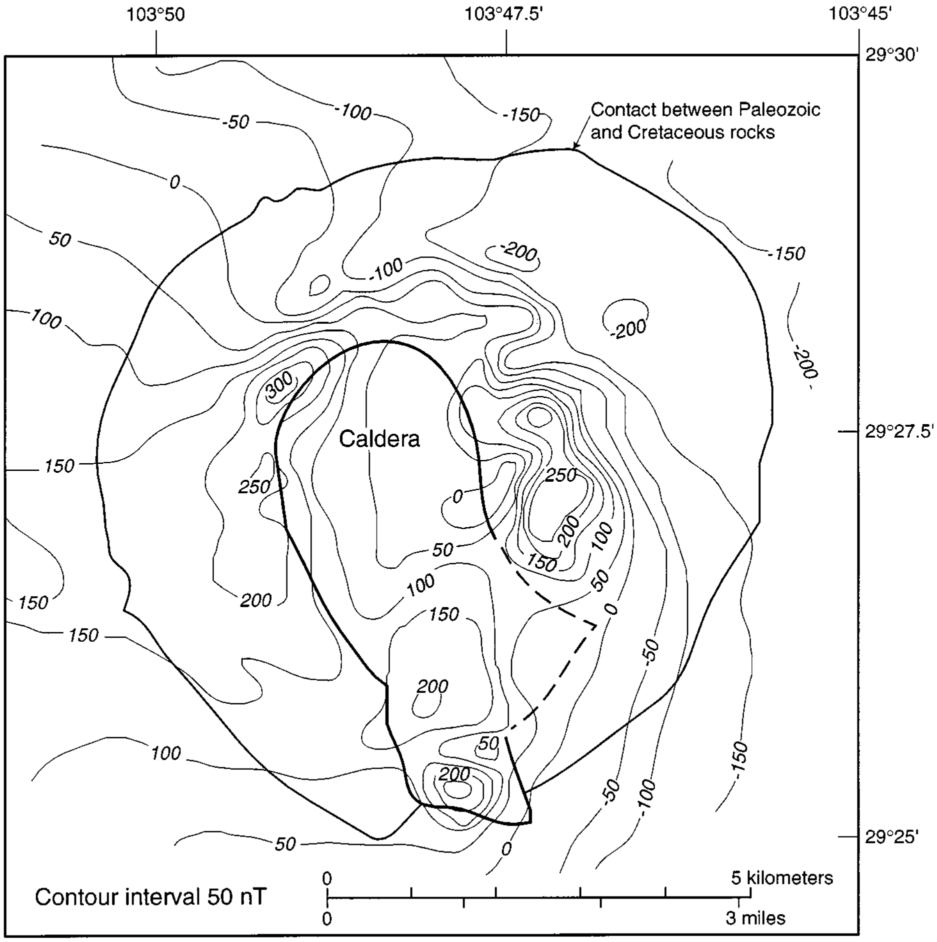

Figure 10. Low-level aeromagnetic map of the Solitario; simplified from map by AMAX Exploration, Inc. and reproduced from Corry et al. (1990). An irregular ring of positive anomalies occurs over the laccolith and a negative anomaly over most of the caldera where the laccolith is thinner by the amount of caldera subsidence. The positive anomaly in the southern part of the caldera coincides with outcrop of ash-flow tuff (Tas), the eruptive product of the laccolith. The negative anomaly immediately north of the tuff coincides with a late porphyritic rhyolite intrusion (Tir5) that may be reversely magnetized. The positive anomaly decreases progressively northward in the caldera, which we interpret to indicate progressive northward thinning of intracaldera ash-flow tuff.

The complexity of evolution and longevity of the Solitario are what are most distinct from traditional laccoliths. Laccoliths typically evolve from an early phase involving emplacement of numerous, stacked sills and small laccoliths (Johnson and Pollard, 1973; Corry, 1988; Jackson and Pollard, 1988). Eventually, one sill grows to a diameter whereby it becomes mechanically easier to lift its roof than to keep growing radially. This body, which may be composed of multiple intrusions, becomes the main laccolith. This progression is generally viewed as a continuum (Corry, 1988). Physical modeling, theoretical considerations of heat loss, and observations of growth of possible historic laccoliths suggest that laccoliths can develop in as

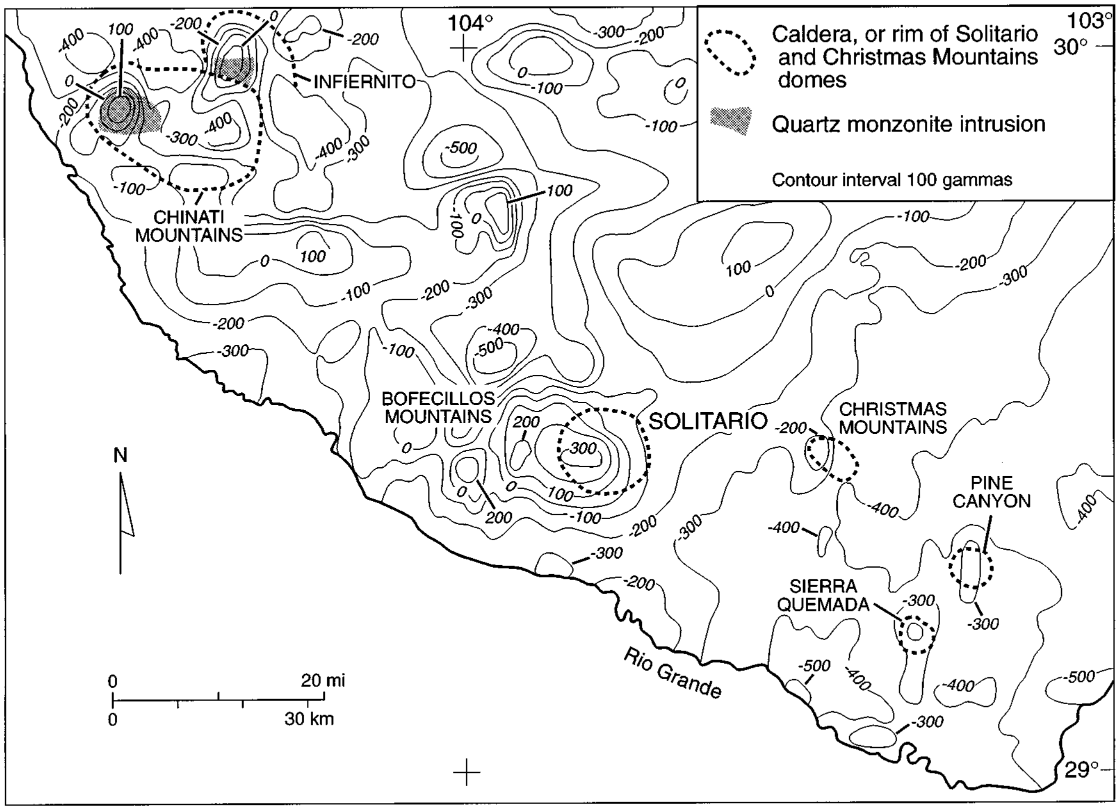

Figure 11. Aeromagnetic map of southern Trans-Pecos Texas (G. Randy Keller, 1993, personal commun.). Positive magnetic anomalies are associated with calderas and other igneous centers, particularly with quartz monzonitic to granitic intrusions within the calderas. These include the Ojo Bonito intrusion of the Infiernito caldera and the West Chinati stock of the Chinati Mountains caldera. The broad positive anomaly associated with the Solitario is consistent with an underlying laccolith of quartz monzonite. Other positive anomalies include several in the Bofecillos Mountains immediately west of the Solitario that probably represent intrusions associated with mafic to intermediate stratovolcanoes, and anomalies south and east of the Chinati Mountains that probably represent uplifted basement.

little as 100 years (Dixon and Simpson, 1987; Corry, 1988; Scaillet et al., 1995).

The Solitario follows the general sequence from initial sill emplacement to growth of a main laccolith. However, the main laccolith is about 0.6 m.y. younger than the initial sills and did not evolve continuously from them. The continuum model may apply to the main pulse, that is, numerous sills may have immediately preceded the main laccolith. These stages probably are continuous in most small laccoliths, but we know of no other studies of the precise timing of sill and laccolith development. Other laccoliths may also have developed episodically.

The further stages of ash-flow eruption, caldera collapse, and late intrusion are particularly uncommon in small laccoliths, although we cite several studies below that relate calderas to laccoliths. In part, this may simply reflect size of the laccolith magma system. Small bodies are unlikely to undergo any sort of complex history. Most laccoliths form clusters, notably in Trans-Pecos Texas (Maxwell et al., 1967) and in the Henry Mountains, Utah, which include several composite domes probably underlain by two or more laccoliths (Gilbert, 1877; Jackson and Pollard, 1988). Complex evolution and long-lived magma systems may be more common but expressed through emplacement of numerous separate laccoliths, rather than through the protracted development of a single laccolith system that we see in the Solitario.

In contrast, the Solitario is comparable in size to many major intrusions that are demonstrably laccoliths, sills, or otherwise floored, tabular bodies. The shape of these intrusions is indicated both from geophysical data for intrusions where the base is not exposed (Bott and Smithson, 1967; Sweeney, 1976; Carrier and Chapman, 1981; Lynn et al., 1981; Carle, 1988; Hodge et al., 1982; Vejmelek and Smithson, 1995; Lyons et al., 1996) and from exposed cross sections (Hamilton and Myers, 1967; Bridgwater et al., 1974; Sides, 1980; Brown et al., 1981; Hildebrand, 1984; Redden et al., 1985; John, 1988; Hogan and Sinha, 1989; Hogan et al., 1992; Hildebrand et al., 1990; Hutton and Ingram, 1992; Guillot et al., 1993; Simony and Halwas, 1993; Scaillet et al., 1995). These examples range from individual plutons a few kilometers to 50 km across and 1 to 5 km thick to batholiths many hundreds of kilometers across and 10 or more km thick. Except for the batholiths, most of the above examples are specifically cited as laccoliths that lifted their roofs. Several of the exposed bodies were fed by dikes, similar to the feeder systems long recognized for small laccoliths (Bridgwater et al., 1974; John, 1988; Brown, 1994; Scaillet et al., 1995). Although the shape of a pluton may vary with the tectonic regime in which it is emplaced, most major intrusions are thin (Marsh, 1989; Bergantz, 1991; Brown, 1994; Vigneresse, 1995). For example, Bergantz (1991) stated that most plutons are 5 to 13 km thick.

Many of these larger bodies intruded along subhorizontal structural discontinuities, which are likely to be much more abundant than horizontal sedimentary rocks except in the shallowest part of the crust. This is an important point regarding our ability to recognize that an intrusion is floored or has domed the intruded rocks. If the Solitario laccolith were exposed approximately midway through its thickness (Fig. 3), it might be difficult to recognize as a laccolith because the Paleozoic host rocks had been highly folded and faulted long before intrusion. Doming of such highly deformed rocks might only be recognized through thorough structural analysis.

Several of the larger laccoliths cited above were emplaced as numerous, thin sills or sheets, rather than as a single large intrusion (Brown et al., 1981; Redden et al., 1985; Nabelek et al., 1992; Guillot et al., 1993; Simony and Halwas, 1993). The Solitario laccolith may also have been emplaced as a series of sheets, and the rim sills definitely constitute a thin version of the "granitic sheets" cited by these authors.

Comparison with Other Calderas

The Solitario is smaller than most conventional ash-flow calderas but, otherwise, exhibits all their characteristics including undergoing long, complex evolution (Smith and Bailey, 1968; Lipman, 1984). Here we emphasize some particularly characteristic features of both the Solitario and calderas in general (excluding calderas associated with stratovolcanoes and shield volcanoes; Wood, 1984).

Caldera Size and Tuff Volume. The Solitario caldera is 6×2 km, whereas calderas are commonly 10 to 30 km in diameter and can range up to more than 80 km (Christiansen, 1979; Smith, 1979; Lipman, 1984; Wood, 1984; Chesner et al., 1991). Other mid-Tertiary calderas in Texas range from 4 to 30 km in diameter (Henry and Price, 1984). Most geologists infer that a caldera is roughly the diameter of the underlying magma chamber (e.g., Smith, 1979; Cas and Wright, 1987). The Solitario caldera is notably smaller than its underlying laccolith. If the Solitario caldera were nearer the diameter of the laccolith, it would be an average-sized caldera. The diameter and depth of emplacement of the laccolith are comparable to those of plutons beneath many conventional calderas.

Similarly, the estimated 2 to 20 km^3 volume of ash-flow tuff in the Solitario is small in comparison to many ash-flow tuffs in Texas and worldwide, which have volumes up to 1000 km^3 (Henry and Price, 1984; Lipman, 1984). Nevertheless, a substantial part of the inferred 90 km^3 of the entire laccolith appears to have erupted.

Duration, Complexity, and Episodicity of Activity. The style, long duration, complexity, and apparent episodicity of Solitario magmatism are much like what are recognized in calderas in general. Specific events in the Solitario match most of those recognized in much larger calderas. Lipman (1984), building upon the resurgent caldera cycle of Smith and Bailey (1968), identified three major divisions of a general caldera cycle: premonitory activity, culminating eruptions and caldera collapse, and postcollapse activity.

Premonitory activity in the Solitario is represented by the rim sills, their related lavas, domes, and tuffs, and the central syenite intrusion of the first pulse. These indicate early development of a magma source that must be much deeper than the main laccolith. These rocks were distinctly less voluminous than the main laccolith and ash-flow tuff. This relation is similar to what is recognized in many calderas, where precollapse volcanism ranges from extensive to, rarely, none, but is generally much less than the culminating ash-flow eruptions (Lipman, 1984). The radial dikes of the main pulse, which we infer were emplaced during initial inflation of the main laccolith and before ash-flow eruption, could also be considered premonitory activity.

Culminating eruptions and caldera collapse are well represented in the Solitario. Ponding of ash-flow tuff within the caldera and its interbedding with megabreccia and debris deposits indicate that caldera collapse occurred contemporaneously with ash-flow eruption, a nearly universal characteristic of major calderas (Smith and Bailey, 1968; Bailey et al., 1976; Lipman, 1976, 1984; Christiansen, 1979; Bacon, 1983; Self et al., 1986; Cas and Wright, 1987). The type and complexity of the caldera-fill sequence are comparable to those seen in much larger calderas. The crudely fining upward sequence of post-tuff deposits indicates that the caldera gradually filled, reducing the gradient from wall to floor. Nevertheless, the prevalence of coarse debris deposits indicates that a moderately steep gradient was always maintained in the small Solitario caldera.

Despite the small volume of erupted tuff, the Solitario caldera collapsed along a single, well-defined ring fracture (Figs. 1 and 3). Exposure and southward dip of the collapse block in the northern part of the caldera indicate that it subsided asymmetrically, but more or less as a coherent block. Possible inward subsidence of Paleozoic rocks across a hinge along the southeastern margin suggests minor, additional complexity. The north-northwest elongation of the Solitario caldera is its only unusual aspect in comparison to larger calderas, which are mostly circular (Lipman, 1984).

Ash-flow vents including a point source and along the ring fracture are well preserved in the Solitario but are rare in the geologic record. Unlike the central vents of many calderas (Bacon, 1983; Lipman, 1984; Hildreth and Mahood, 1986; Self et al., 1986), the point vent in the Solitario is central to neither the caldera nor to the underlying laccolith. The vent may have been localized along a Paleozoic fault that was reactivated during doming. The ring-fracture vents are more poorly preserved, probably as a result of disruption during caldera collapse (Lipman, 1984). The relative timing of the Solitario vents is unknown. Initial eruption through a central vent followed by development of a ring fracture as collapse began is postulated for several calderas (Bacon, 1983; Hildreth and Mahood, 1986; Self et al., 1986), but these central vents are buried beneath caldera fill and not observed directly. Possible mechanisms to trigger ash-flow eruption include failure of the roof related to magma buildup and disruption of the magma chamber related to regional tectonism (Lipman et al., 1984). For the Solitario, inflation of the laccolith caused extreme doming, extension, and fracturing over the magma chamber. The observed amount of doming indicates extension of about 8%, or 1.2 km, at the base of Cretaceous rocks. Fractures probably propagated to the chamber and allowed it to erupt. In contrast, regional tectonism was not a factor because no tectonic faulting occurred at this time in Texas (Henry et al., 1991).

Possibly the most unusual aspect of the Solitario is its extreme precollapse doming. Although regional tumescence, the development of a structural dome over the caldera magma body, was initially considered a characteristic of calderas (Smith and Bailey, 1968), tumescent doming is, at most, gentle around most calderas (Smith and Bailey, 1968; Christiansen et al., 1977; Lipman, 1984; Henry and Price, 1984). One exception is the 30×20 km Chinati Mountains caldera of Texas, where precaldera rocks along the southern margin dip outward from 30° to 40° (Cepeda and Henry, 1983; Henry and Price, 1984). Several factors may act to reduce surface doming or mask minor doming around many calderas. Some of the space for both shallow and deep laccoliths is probably taken up by downbowing of underlying crust (Pollard and Johnson, 1973; Bridgwater et al., 1974; Corry, 1988; Brown, 1994), so doming may be less than the thickness of the intrusion. For example, the 30×25 km Timber Mountain caldera, Nevada, is an example of a caldera with gentle (≤10°) precollapse doming, which Christiansen et al. (1977) ascribed to "magmatic insurgence." Although other magma body shapes are possible, such doming is consistent with an underlying laccolith. The 23×17 km Grizzly Peak caldera of Colorado is not obviously domed, but has an arcuate ring of cone-sheet dikes that is interpreted to indicate uplift over a "batholith-sized sill, about 25 km in diameter and perhaps 10 km below the surface" (Fridrich et al., 1991). Slumping of the caldera wall during ash-flow eruption and collapse greatly widens the apparent caldera, so that the caldera topographic margin extends well beyond its underlying structural margin

(Lipman, 1984). Much of the domed area may cave into the caldera through this process. Many calderas erupt through early-formed ring fractures (Lipman, 1984; Hildreth and Mahood, 1986). Some ring fractures may develop in response to initial collapse following eruption from a central vent, but Smith and Bailey (1968) argued that ring fractures largely reflect doming preceding ash-flow eruption. In any event, extension resulting from doming over a laccolith would allow a caldera block to subside regardless of whether ring faults dipped inward or outward (Lipman, 1984; Branney, 1995).

Postcollapse activity is represented by the intracaldera trachyte lava and by numerous intrusions in and around the caldera. Multiple episodes of intracaldera or ring-fracture intrusion and volcanism are characteristic of calderas worldwide (Smith and Bailey, 1968; Lipman, 1984). For example, detailed study of the three large, young calderas of the western United States (Long Valley, California; Yellowstone National Park; and Valles, New Mexico) demonstrates that postcollapse rhyolite domes, flows, and pyroclastic rocks erupted in brief episodes spread over about 1 m.y. and separated by repose times of several hundred thousand years (Bailey et al., 1976; Hildreth et al., 1984; Spell et al., 1993). Postcollapse activity in the Solitario could have occurred in a single episode at 35.0 Ma, but most of the late intrusions are undated.

The Solitario underwent late subsidence of the caldera block, between 35.4 and 35.0 Ma, rather than resurgence. Subsidence may be related to eruption of late, small-volume tuffs that are present in upper parts of caldera fill, but the cause is uncertain. Similar late subsidence occurred in several other small calderas in Texas (Henry and Price, 1984) and appears to be particularly characteristic of, but not restricted to, small calderas (Lipman, 1984; Marsh, 1984; Walker, 1984; Branney, 1995). The abundant small intrusions of the final pulse represent a significant, postcollapse magmatic event that may be equivalent to resurgence (Elston, 1984).

Although the volume of Solitario magmas is modest in comparison to that of most calderas, activity persisted for at least 1 m.y. The main laccolith could not exist as a magma source for even a small fraction of this time. Therefore, the complex, episodic development requires recurrent magma generation and rise from a deeper source. On the basis of petrographic similarities of Solitario rocks, these magmas were probably chemically similar throughout its history. Our speculation that the Terneros Creek Rhyolite is a crustal melt related to the Solitario system further suggests a major heat anomaly at depth, which may have existed throughout Solitario activity. Similar, extended activity and replenishment from a deep source has been interpreted from age and geochemical data for both larger calderas and laccolith complexes (Hildreth, 1981; Nabelek et al., 1992; Spell et al., 1993). For example, Nabelek et al. (1992) interpreted geochemical data to indicate that the Harney Peak Granite, a sill and dike complex, developed through repeated injections of magma from two distinct crustal sources. Although Nabelek et al. (1992) called upon multiple diapirs for magma emplacement, Brown (1994) argued that the sills were more likely fed by dikes, the mechanism for laccoliths in general.

Other Laccocalderas

The Solitario laccocaldera is not unique. Although not prominent in the literature, several other calderas related to laccoliths have been identified, and floored intrusions are interpreted to underlie many other calderas. The Solitario is one of five definite or probable laccocalderas in Texas and adjacent Mexico (Henry and Price, 1989). The Christmas Mountains laccocaldera (Fig. 11), the most thoroughly studied, has an 8 × 5 km dome, erupted a complex sequence of ash-flow tuffs, and developed several small calderas (Henry and Price, 1989).

Outside of Texas, the best and largest examples of calderas underlain by laccoliths are exposed in deeply dissected folds of the 1.9 Ga Great Bear magmatic zone of the Canadian Shield (Hildebrand, 1984; Hildebrand et al., 1990). Calderas there are up to 20 km across and underlain by sills or laccoliths up to several tens of kilometers in diameter and 1 to 4 km thick. As in Texas, these ancient laccocalderas underwent contemporaneous ash-flow eruption and caldera collapse and are filled by thick sequences of tuff, interbedded breccia, and postcollapse lava and sedimentary rock. Resurgent quartz monzonitic plutons intruded the core of the tuff sequences.

Several calderas are interpreted to have either laccolithic magma chambers or resurgent intrusions. The deep, batholithic sill of the Grizzly Peak caldera is an excellent example of the former (Fridrich et al., 1991). Resurgent intrusions in this caldera and others in California, Colorado, Arizona, and Texas are also considered to be laccoliths (Lambert et al., 1987; Hon and Fridrich, 1989; du Bray and Pallister, 1991; Fridrich et al., 1991; Henry et al., 1992). Calderas in the St. Francois Mountains of Missouri are underlain by tabular plutons (Sides, 1980; Sides et al., 1981), which may be either the original caldera magma chamber or resurgent bodies. Gravity data indicate that the Long Valley caldera of California is underlain by a 16-km-wide, 7-km-thick silicic pluton (Carle, 1988), although Iyer et al. (1990) interpreted this to be only the upper part of a thicker body. McConnell et al. (1995) interpret resurgence of the Long Valley caldera to have resulted from emplacement of numerous rhyolitic sills within intracaldera Bishop Tuff, rather than from inflation of the magma chamber.

Other probable, eruptive laccoliths include the Alid volcanic center, Eritrea, northeast Africa (Clynne et al., 1996; Duffield et al., 1996), Drake Peak, Oregon (Wells, 1979), and Gross Brukkaros, Namibia (Stachel et al., 1994). Alid is a young (active?), 7 × 5 km, at least 1-km-high structural dome with dips ranging from 25° to 65° that probably overlies a laccolith (Clynne et al., 1996; Duffield et al., 1996). A 3 × 2 km collapse area occupies the summit of the dome. Rhyolitic lavas erupted from the center of the dome immediately before doming. Following doming, 1 to 5 km^3 of rhyolitic tuff erupted from the west end of the summit, partly filled the collapse area, and blanketed much of the dome and some surrounding areas. Clynne et al. (1996) interpreted collapse to have resulted from extension over the dome, not from caldera collapse. However, the substantial volume of tuff relative to size of the dome would seem to require some caldera collapse. Alid shows similar volcanic evolution to the Solitario and may be a particularly young laccocaldera.

The Drake Peak rhyolite center of southeastern Oregon is a 9-km-wide structural dome that erupted late rhyolite lavas but no tuff (Wells, 1979). Although Wells attributed doming to a stock-like body, the geometry of the dome suggests a laccolith. Predoming rocks are tilted radially outward between 35° and 60°. The dome is cut by radial faults, and a crestal graben occupies the center of the dome. Rhyolite lava erupted across the southern flank of the dome after uplift. Drake Peak appears to be a laccolith-volcanic complex but not a caldera.

Gross Brukkaros in Namibia appears to be a particularly unusual laccolith-caldera system (Stachel et al., 1994). Gross Brukkaros has a 3-km-diameter, circular, central depression developed within a dome that is 10 km wide and 400 m high. Debris-flow, fluvial, and lacustrine deposits partly fill the depression. Stachel et al. interpreted these relations to indicate central subsidence without ring faults over an alkaline laccolith. Although the apparent caldera contains no primary pyroclastic deposits, Stachel et al. (1994) related subsidence to venting of the laccolith through several diatremes that ring the structure.

The model of batholiths as thin sheets that intrude their own volcanic ejecta (Hamilton and Myers, 1967) has some similarities to laccocalderas. Although Hamilton and Myers envision batholiths breaching the surface and do not discuss doming of intruded rocks, their Figure 4 specifically depicts calderas over thin batholiths.

The sizes of many calderas indicate that they must have developed over floored, tabular intrusions. Magma chambers are inferred to be approximately the same diameter as their calderas (Smith, 1979; Lipman, 1984; Cas and Wright, 1987). Many calderas are more than 30 km in diameter, and the largest are as much as 80 km in diameter (Christiansen, 1979; Smith, 1979; Lipman, 1984; Chesner et al., 1991). For example, the Huckleberry Ridge and Yellowstone calderas of the Yellowstone Plateau are more than 80 km in diameter and 65 × 45 km, respectively (Christiansen, 1979; Hildreth et al., 1984). Recent reexamination of La Garita caldera of the San Juan Mountains, Colorado, shows that it is 70 × 30 km (Lipman et al., 1996). Magma chambers this deep would extend well into the upper mantle, an obvious impossibility. Therefore, they must be much wider than they are deep.

Certainly, many intrusions are not subhorizontal sheets (Pitcher, 1979; Barnes et al., 1986; Lyons et al., 1996), and many calderas must be underlain by thick intrusions (John, 1995; Lipman et al., 1996). The shape of the magma chamber beneath most calderas is unknown. Nevertheless, the many examples above demonstrate that calderas are commonly underlain by laccoliths or other floored intrusions.

Granite Space Problem

Laccolithic emplacement of the Solitario and other intrusions has implications for the revived "room" problem for granitic bodies. Although laccolithic intrusion and doming of host rocks is cited as a possible resolution (Clemens and Mawer, 1992; Brown, 1994; Petford, 1996), a common view appears to be that space for plutons, including laccoliths, is made by emplacement into contemporaneously active fault zones (Hutton, 1988, 1992; Guillot et al., 1993; Hanson and Glazner, 1995; Scaillet et al., 1995). Paterson and Fowler (1993) have challenged the faulting-emplacement mechanism, and we suggest that laccolithic emplacement may be common.

The Solitario formed during a tectonically neutral period in Texas following Laramide folding, which ended about 50 Ma, and preceding Basin and Range faulting, which began at about 24 Ma (Henry et al., 1991). At least 14 other calderas, ranging up to 30 km in diameter and presumably underlain by magma chambers of similar diameter, formed in Texas and adjacent Chihuahua, Mexico, between 42 and 28 Ma (Henry and Price, 1984; Henry et al., 1991). Faulting during this period was insignificant and related only to emplacement of the caldera magma bodies. Therefore, space for these bodies cannot have been generated by contemporaneous faulting. Space for the Solitario was made by doming overlying rock, and possibly by subsidence beneath the laccolith, which commonly occurs beneath sills and shallow laccoliths (Pollard and Johnson, 1973) and possibly beneath mid-crustal intrusions (Bridgwater et al., 1974; Brown, 1994). Many other calderas also formed in areas that underwent little if any faulting. For example, the San Juan caldera field of Colorado, one of the best documented (Lipman, 1984), developed before and during earliest Basin and Range extension. However, total extension in the San Juan field is negligible, so space for the underlying batholith did not come from faulting. We do not argue that all intrusions are laccoliths, only that contemporaneous faulting is not generally necessary.

Laccocaldera Model

Figure 12 depicts the possible geometry and evolution of a large laccocaldera. The surface expression of a laccocaldera is unlikely to be markedly different from that of a caldera that developed over a more stocklike body. The dimensions of the caldera, area of the underlying laccolith, volume of both intracaldera and outflow tuff, amount of collapse, and potential for resurgence are all consistent with descriptions of calderas (Lipman, 1984). Vertical compositional zoning, a common characteristic of caldera magma chambers, could develop in a laccolith. The laccolithic origin might be recognizable only if precollapse rocks were recognizably domed. The laccolithic caldera magma chamber and resurgent intrusions would be fed by dikes, which is an efficient way to transport granitic magma from depth and generate large plutons (Clemens and Mawer, 1992; Hutton, 1992; Petford et al., 1993; Petford, 1996).

Certainly magma bodies beneath calderas can be emplaced by other mechanisms and have different shapes. Alternative ascent or emplacement mechanisms include diapirism, ballooning plutons, intrusion into active fault zones, and stoping. It is far beyond the scope of this report to address these other possibilities. Emplacement mechanisms of plutons are highly controversial; each has its supporters and detractors (Marsh, 1984; Hutton, 1988; Mahon et al., 1988; Clemens and Mawer, 1992; Brown, 1994; Hanson and Glazner, 1995; Paterson and Fowler, 1993, 1995; Vigneresse, 1995; Morgan and Law, 1996; Petford, 1996). Possibly each is effective in specific circumstances. Nevertheless, laccolith emplacement is increasingly cited (Petford, 1996), including for bodies previously interpreted as diapirs or ballooned plutons (Morgan and Law, 1996). We are unwilling even to speculate on the percentage of calderas underlain by laccoliths, but the abundance of major intrusions as laccoliths suggests that laccocalderas are probably common.

Our conclusion that the surface expression of a laccocaldera is likely to be similar to that of a caldera developed over a more spherical or tall, cylindrical body makes identifying diagnostic characteristics of laccocalderas difficult. Potentially fruitful lines of inquiry may come from structural analysis of precaldera rocks, from evaluation of the regional tectonic setting of a caldera, and from experimental studies of caldera development. Precaldera doming could develop over a laccolith, a ballooned pluton, or a diapir. However, doming may be most common over a laccolith. Calderas are shallow crustal features; doming as a space-making process is most effective in the shallow crust (Paterson and Fowler, 1995). Diapirs may be restricted to deep parts of the crust (Mahon et al., 1988). Ballooned plutons are somewhat similar to laccoliths in that magma is interpreted to rise through dikes and expand at the final emplacement level (Paterson and Fowler, 1995). However, ballooned plutons expand radially and symmetrically.

Knowledge of the tectonic regime in which a caldera formed can at least narrow the possible emplacement mechanisms. Laccoliths, diapirs, and ballooned plutons can probably develop in any tectonic setting, whereas the faulting-emplacement mechanism requires major faulting contemporaneous with caldera development.

Experimental studies of caldera development may help evaluate the shape of underlying magma chambers but are currently few. Laccolithic-looking domes developed over both tabular and spherical bodies inflated at shallow depth (Komuro, 1987; Marti et al., 1994). Marti et al. (1994) modeled both spherical and more tabular bodies, but did not indicate the aspect ratio of the tabular bodies, so the significance of their results for laccocalderas is uncertain.

CONCLUSIONS

The Solitario is a complex laccocaldera that developed in at least three distinct stages at 36.0, 35.4, and 35.0 Ma. Numerous sills, dikes, and small laccoliths and related volcanic rocks were emplaced during the first pulse. During the second, main pulse, emplacement of the main laccolith uplifted the 16-km-diameter Solitario dome. Contemporaneously, dikes intruded along radial fractures as the dome grew, voluminous ash-flow tuff erupted, and a 6 × 2–km-diameter caldera formed across the top of the dome. The caldera was filled by a complex sequence of megabreccia, debris deposits, and minor trachyte lava, probably shortly after collapse, and then underwent late subsidence. During the final pulse, numerous dikes and small laccoliths intruded caldera fill or along the caldera ring fracture. This complex evolution is similar to that recognized in much larger

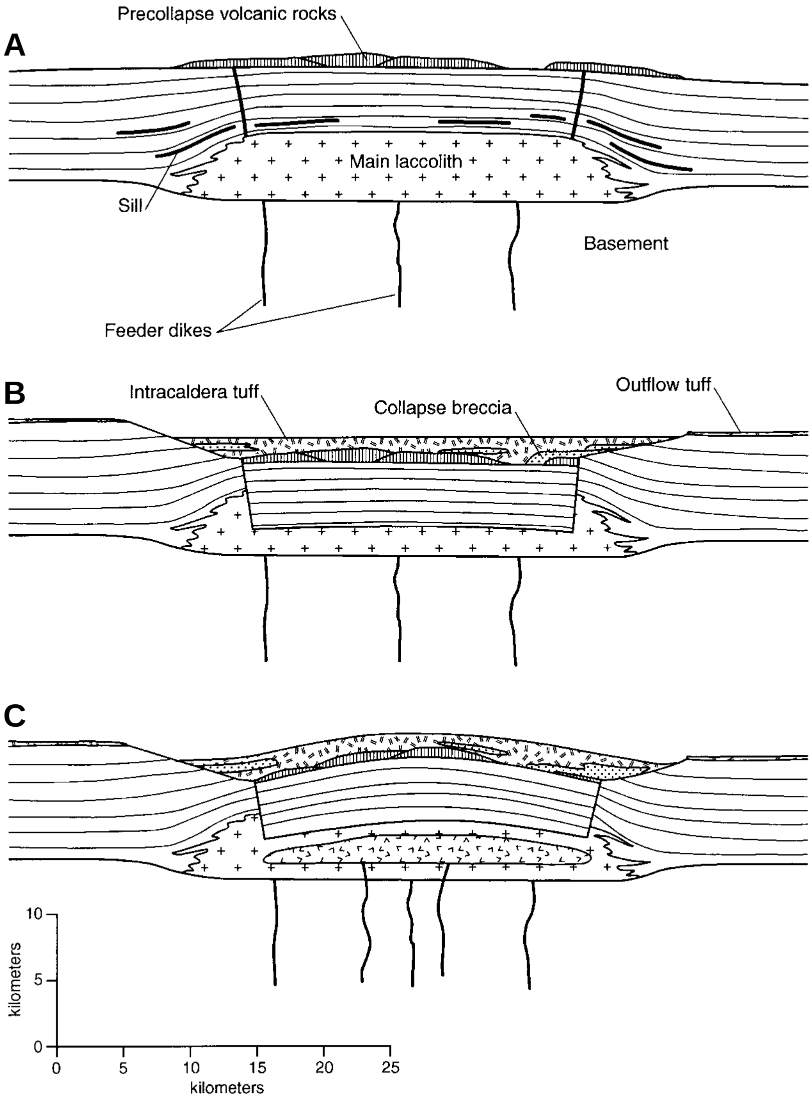

Figure 12. The laccocaldera model of caldera development, based on the geology of the Solitario and on published data, especially Lipman (1984). This caldera has all the characteristics of conventional calderas and probably could not be easily identified as a laccocaldera. (A) A large laccolith, fed by dikes from a deeper source, intrudes along a subhorizontal horizon at a depth of approximately 5 km; in many cases, this horizon may be a structural discontinuity rather than a sedimentary layer. The laccolith is 5 km thick and 30 to 35 km across and has a volume of approximately 4000 km^3. Space for the laccolith is made partly by uplifting overlying rocks and partly by subsidence of underlying crust. The amount of doming decreases upward and is distributed over a wider area. The laccolith could, but need not, consist of numerous individual sills, and several sills intrude stratified rocks above and around it. Contemporaneously, minor lavas and tuffs erupt over the laccolith. Fractures develop above the laccolith, particularly along the zone of maximum bending of host rock near its edges. These eventually tap the magma chamber and allow ash-flow eruption. (B) Immediately after ash-flow eruption and caldera collapse. Eruption of approximately 1250 km^3 of tuff induces about 2.5 km collapse of the caldera block. Approximately 1.5 km (about 750 km^3) of tuff ponds within the caldera and is interstratified with breccias slumped from the caldera wall. Another 500 km^3 of tuff is deposited as an outflow sheet. Larger volumes of tuff could be generated by increasing the size or thickness of the laccolith or by allowing greater collapse. Slumping of the wall and burial beneath tuff and breccia disguises much of the evidence for precaldera doming. (C) Resurgence. A late pulse of magma rises along dikes from the deeper source and intrudes the original laccolithic caldera magma chamber, uplifting the caldera block approximately 2 km. Published descriptions indicate that this resurgent intrusion could be composite and emplaced at any level up to and including within intracaldera tuff.

calderas. The extended, episodic activity requires repeated injections of magma from a deep source, well below the level of the main laccolith.

Published reports indicate that many large intrusions are laccoliths and that several calderas are underlain by laccoliths. Experimental and observational data indicate that large plutons are fed by dikes and can and should generally be floored, tabular bodies. Laccolithic intrusion is probably a common way to solve the space problem for plutons; concurrent faulting may have provided space for some plutons but is not universally necessary. We propose that many calderas are underlain by laccoliths or other floored intrusions.

ACKNOWLEDGMENTS

Mapping of the Solitario was supported by the Texas Parks and Wildlife Department (IAC No. 90-91-1267 and 92-93-0741) and the U.S. Geological Survey COGEOMAP program (agreement numbers 14-08-0001-A0811, 14-08-0001-A0890, and 1434-92-A-1086). We thank Jon Price and Don Noble for discussions and reviews of an early draft, and Peter Lipman, Gary Smith, and Marie Jackson for thorough, constructive reviews of the submitted manuscript.

REFERENCES CITED

Alexander, E. C., Jr., Mickelson, G. M., and Lanphere, M. A., 1978, MMhb-1: A new ^{40}Ar/^{39}Ar dating standard, *in* Zartman, R. E., ed., Short papers of the Fourth International Conference, Geochronology, Cosmochronology, Isotope Geology 1978: U.S. Geological Survey Open-File Report 78-701, p. 6–8.

Bacon, C. R., 1983, Eruptive history of Mount Mazama and Crater Lake caldera, Cascade Range, U.S.A.: Journal of Volcanology and Geothermal Research, v. 18, p. 57–115.

Bailey, R. A., Dalrymple, G. B., and Lanphere, M. A., 1976, Volcanism, structure, and geochronology of Long Valley caldera, Mono County, California: Journal of Geophysical Research, v. 81, p. 725–744.

Barnes, C. G., Rice, J. M., and Gribble, R. F., 1986, Tilted plutons in the Klamath Mountains of California and Oregon: Journal of Geophysical Research, v. 91, p. 6059–6071.

Bates, R. L., and Jackson, J. A., 1987, Glossary of geology: Alexandria, Virginia, American Geological Institute, 788 p.

Bergantz, G. W., 1991, Physical and chemical characterization of plutons: Reviews in Mineralogy, v. 26, p. 13–42.

Bott, M. P. H., and Smithson, S. B., 1967, Gravity investigations of subsurface shape and mass distributions of granite batholiths: Geological Society of America Bulletin, v. 78, p. 859–878.

Branney, M. J., 1995, Downsag and extension at calderas: New perspectives on collapse geometries from ice-melt, mining, and volcanic subsidence: Bulletin Volcanology, v. 57, p. 303–318.

Bridgwater, D., Sutton, J., and Watterson, J., 1974, Crustal downfolding associated with igneous activity: Tectonophysics, v. 21, p. 57–77.

Brown, M., 1994, The generation, segregation, ascent and emplacement of granite magma: The migmatite-to-crustally derived granite connection in thickened orogens: Earth-Science Reviews, v. 36, p. 83–130.

Brown, M., Friend, C. R. L., McGregor, V. R., and Perkins, W. T., 1981, The late-Archaean Qorqut granite complex of southern west Greenland: Journal of Geophysical Research, v. 86, p. 10617–10632.

Carle, S. F., 1988, Three-dimensional gravity modeling of the geologic structure of Long Valley caldera: Journal of Geophysical Research, v. 93, p. 13237–13250.

Carrier, D. L., and Chapman, D. S., 1981, Gravity and thermal models for the Twin Peaks silicic volcanic center, southwestern Utah: Journal of Geophysical Research, v. 86, p. 10287–10302.

Cas, R. A. F., and Wright, J. V., 1987, Volcanic successions: Modern and ancient: London, Allen and Unwin, 528 p.

Cathles, L. M., 1981, Fluid flow and genesis of hydrothermal ore deposits: Economic Geology, 75th Anniversary Volume, p. 424–457.

Cepeda, J. C., and Henry, C. D., 1983, Oligocene volcanism and multiple caldera formation in the Chinati Mountains, Presidio County, Texas: University of Texas at Austin, Bureau of Economic Geology Report of Investigations 135, 32 p.

Chesner, C. A., Rose, W. I., Deino, A., Drake, R., and Westgate, J. A., 1991, Eruptive history of Earth's largest Quaternary caldera (Toba, Indonesia) clarified: Geology, v. 19, p. 200–203.

Christiansen, R. L., 1979, Cooling units and composite sheets in relation to caldera structure, in Chapin, C. E., and Elston, W. E., eds., Ash-flow tuffs: Geological Society of America Special Paper 180, p. 29–42.

Christiansen, R. L., Lipman, P. W., Carr, W. J., Byers, F. M., Jr., Orkild, P. P., and Sargent, K. A., 1977, Timber Mountain–Oasis Valley caldera complex of southern Nevada: Geological Society of America Bulletin, v. 88, p. 943–959.

Clemens, J. D., and Mawer, C. K., 1992, Granitic magma transport by fracture propagation: Tectonophysics, v. 204, p. 339–360.

Clynne, M. A., and nine others, 1996, Geology and geothermal potential of Alid volcanic center, Eritrea, Africa: Geothermal Resources Council Transactions, v. 20, p. 279–286.

Corry, C. E., 1988, Laccoliths: Mechanics of emplacement and growth: Geological Society of America Special Paper 220, 120 p.

Corry, C. E., Herrin, E., McDowell, F. W., and Phillips, K. A., 1990, Geology of the Solitario, Trans-Pecos Texas: Geological Society of America Special Paper 250, 122 p.

Daly, R. A., 1933, Igneous rocks and the depths of the Earth: New York, Hafner Publishing, 598 p.

Dalrymple, G. B., Alexander, E. C., Jr., Lanphere, M. A., and Kraker, G. P., 1981, Irradiation of samples for $^{40}Ar/^{39}Ar$ dating using the Geological Survey TRIGA reactor: U.S. Geological Survey Professional Paper 1176, 55 p.

Dixon, J. M., and Simpson, D. G., 1987, Centrifuge modeling of laccolith intrusion: Journal of Structural Geology, v. 9, p. 87–103.

Druitt, T. H., and Sparks, R. S. J., 1984, On the formation of calderas during ignimbrite eruptions: Nature, v. 310, p. 679–681.

du Bray, E. A., and Pallister, J. S., 1991, An ash flow caldera in cross section: Ongoing field and geochemical studies of the mid-Tertiary Turkey Creek caldera, Chiricahua Mountains, SE Arizona: Journal of Geophysical Research, v. 96, p. 13435–13457.

Duffield, W. A., Jackson, M. D., Smith, J. G., Lowenstern, J. B., and Clynne, M. A., 1996, Structural doming over an upper crustal magma body at Alid, Eritrea: Eos (Transactions, American Geophysical Union), v. 77, p. F792.

Elston, W. E., 1984, Mid-Tertiary ash flow tuff cauldrons, southwestern New Mexico: Journal of Geophysical Research, v. 89, p. 8733–8750.

Erdlac, R. J., Jr., 1990, A Laramide-age push-up block: The structures and formation of the Terlingua-Solitario structural block, Big Bend region, Texas: Geological Society of America Bulletin, v. 102, p. 1065–1076.

Fleck, R. J., Sutter, J. F., and Elliott, D. H., 1977, Interpretation of discordant $^{40}Ar/^{39}Ar$ age-spectra of Mesozoic tholeiites from Antarctica: Geochimica et Cosmochimica Acta, v. 41, p. 15–32.

Fridrich, C. J., Smith, R. P., DeWitt, E., and McKee, E. H., 1991, Structural, eruptive, and intrusive evolution of the Grizzly Peak caldera, Sawatch Range, Colorado: Geological Society of America Bulletin, v. 103, p. 1160–1177.

Gilbert, G. K., 1877, Report on the geology of the Henry Mountains: U.S. Geographical and Geological Survey, Rocky Mountains region, 170 p.

Guillot, S., Pecher, A., Rochette, P., and Le Fort, P., 1993, The emplacement of the Manaslu granite of central Nepal: Field and magnetic susceptibility constraints, *in* Treloar, P. J., and Sealre, M. P., eds., Himalayan tectonics: Geological Society [London] Special Publication 74, p. 413–428.

Hamilton, W., and Myers, W. B., 1967, The nature of batholiths: U.S. Geological Survey Professional Paper 554-C, 30 p.

Hanson, R. B., and Glazner, A. F., 1995, Thermal requirements for extensional emplacement of granitoids: Geology, v. 23, p. 213–216.

Haugerud, R. A., and Kunk, M. J., 1988, ArAr*, a computer program for reduction of $^{40}Ar/^{39}Ar$ data: U.S. Geological Survey Open-File Report 88-261, 68 p.

Henry, C. D., 1996, Igneous geology of the Solitario, *in* Henry, C. D., and Muehlberger, W. R., eds., Geology of the Solitario Dome, Trans-Pecos Texas: Paleozoic, Mesozoic, and Cenozoic sedimentation, tectonism, and magmatism: University of Texas at Austin, Bureau of Economic Geology, Report of Investigations 240, p. 57–80.

Henry, C. D., and Kunk, M. J., 1996, Geochronology of the Solitario and adjacent volcanic rocks, *in* Henry, C. D., and Muehlberger, W. R., eds., Geology of the Solitario Dome, Trans-Pecos Texas: Paleozoic, Mesozoic, and Cenozoic sedimentation, tectonism, and magmatism: University of Texas at Austin, Bureau of Economic Geology, Report of Investigations 240, p. 109–120.

Henry, C. D., and McDowell, F. W., 1986, Geochronology of the mid-Tertiary volcanic field, Trans-Pecos Texas, *in* Price, J. G., Henry, C. D., Parker, D. F., and Barker, D. S., eds., Igneous geology of Trans-Pecos Texas: University of Texas at Austin, Bureau of Economic Geology Guidebook 23, p. 99–122.

Henry, C. D., and Muehlberger, W. R., 1996, Geology of the Solitario Dome, Trans-Pecos Texas: Paleozoic, Mesozoic, and Cenozoic sedimentation, tectonism, and magmatism: University of Texas at Austin, Bureau of Economic Geology Report of Investigations 240, 182 p.

Henry, C. D., and Price, J. G., 1984, Variations in caldera development in the Tertiary volcanic field of Trans-Pecos Texas: Journal of Geophysical Research, v. 89, p. 9765–8786.

Henry, C. D., and Price, J. G., 1989, The Christmas Mountains caldera complex, Trans-Pecos Texas: The geology and development of a laccocaldera: Bulletin of Volcanology, v. 52, p. 97–112.

Henry, C. D., Price, J. G., and James, E. W., 1991, Mid-Cenozoic stress evolution and magmatism in the southern Cordillera, Texas and Mexico: Transition from continental arc to intraplate extension: Journal of Geophysical Research, v. 96, p. 13545–13560.

Henry, C. D., Price, J. G., Duex, T. W., and James, E. W., 1992, Geology of the Infiernito caldera and magmatic evolution of the Chinati Mountains caldera complex, Trans-Pecos Texas: University of Texas at Austin, Bureau of Economic Geology Report of Investigations 206, 56 p.

Henry, C. D., Muehlberger, W. R., Erdlac, R. J., Jr., Price, J. G., and Dickerson, P. W., 1994, Discussion of Special Paper 250 "Geology of the Solitario, Trans-Pecos Texas": Geological Society of America Bulletin, v. 106, p. 560–569.

Henry, C. D., Davis, L. L., Kunk, M. J., and McIntosh, W. C., 1997, Tertiary volcanism of the Bofecillos Mountains and Big Bend Ranch State Natural Area: Revised stratigraphy and $^{40}Ar/^{39}Ar$ geochronology: University of Texas at Austin, Bureau of Economic Geology, Report of Investigations (in press).

Herrin, E. T., 1957, Geology of the Solitario area, Trans-Pecos Texas [Ph.D. dissert.]: Cambridge, Massachusetts, Harvard University, 162 p.

Hildebrand, R. S., 1984, Folded cauldrons of the Early Proterozoic Labine Group, northwestern Canadian Shield: Journal of Geophysical Research, v. 89, p. 8429–8440.

Hildebrand, R. S., Bowring, S. A., and Housh, T., 1990, Sheet-like epizonal plutons in the Great Bear magmatic zone, northwestern Canadian Shield: Geological Society of America Abstracts with Programs, v. 22, no. 7, p. A244.

Hildreth, W., 1981, Gradients in silicic magma chambers: Implications for lithospheric magmatism: Journal of Geophysical Research, v. 86, p. 10153–10193.

Hildreth, W., and Mahood, G. A., 1986, Ring-fracture eruption of the Bishop Tuff: Geological Society of America Bulletin, v. 97, p. 396–403.

Hildreth, W., Christiansen, R. L., and O'Neil, J. R., 1984, Catastrophic isotopic modification of rhyolitic magma at times of caldera subsidence, Yellowstone Plateau volcanic field: Journal of Geophysical Research, v. 89, p. 8339–8369.

Hodge, D. S., Abbey, D. A., Harbin, M. A., Patterson, J. L., Ring, M. J., and Sweeney, J. F., 1982, Gravity studies of subsurface mass distributions of granitic rocks in Maine and New Hampshire: American Journal of Science, v. 282, p. 1289–1324.

Hogan, J. P., and Sinha, A. K., 1989, Compositional variation of plutonism in the coastal Maine magmatic province: Mode of origin and tectonic setting, *in* Tucker, R. D., and Marvinney, R. G., eds., Studies in Maine geology: Augusta, Maine Geological Survey, v. 4, p. 1–33.

Hogan, J. P., Gilbert, M. C., Weaver, B. L., and Myers, J. D., 1992, High-level A-type sheet granites of the Wichita Mountains igneous province, Oklahoma, U.S.A., *in* Brown, P. E., and Chappell, B. W., eds., The second Hutton symposium on the origin of granites and related rocks: Geological Society of America Special Paper 272, p. 491–492.

Hon, K., and Fridrich, C. J., 1989, How calderas resurge: New Mexico Bureau of Mines and Mineral Resources, Bulletin 131, Continental magmatism abstracts, p. 135.

Hutton, D. H. W., 1988, Granite emplacement mechanisms and tectonic controls: Inferences from deformation studies: Royal Society of Edinburgh Transactions, Earth Sciences, v. 79, p. 245–255.

Hutton, D. H. W., 1992, Granite sheeted complexes: Evidence for the diking ascent mechanism, *in* Brown, P. E., and Chappell, B. W., eds., The second Hutton symposium on the origin of granites and related rocks: Geological Society of America Special Paper 272, p. 377–382.

Hutton, D. H. W., and Ingram, G. M., 1992, The Great Tonalite sill of southeastern Alaska and British Columbia: Emplacement into an active contractional high angle reverse shear zone, *in* Brown, P. E., and Chappell, B. W., eds., The second Hutton symposium on the origin of granites and related rocks: Geological Society of America Special Paper 272, p. 383–386.

Hyndman, D. W., and Alt, D., 1987, Radial dikes, laccoliths, and gelatin models: Journal of Geology, v. 95, p. 763–774.

Iyer, H. M., Evans, J. R., Dawson, P. B., Stauber, D. A., and Achauer, U., 1990, Differences in magma storage in different volcanic environments as revealed by seismic tomography: Silicic volcanic centers and subduction-related volcanoes, *in* Ryan, M. P., ed., Magma transport and storage: New York, John Wiley, p. 293–316.

Jackson, M. D., and Pollard, D. D., 1988, The laccolith-stock controversy: New results from the southern Henry Mountains, Utah: Geological Society of America Bulletin, v. 100, p. 117–139.

James, E. W., and Henry, C. D., 1991, Compositional changes in Trans-Pecos Texas magmas coincident with Cenozoic stress realignment: Journal of Geophysical Research, v. 96, p. 13561–13576.

James, E. W., and Henry, C. D., 1993, Southeastern extent of the North American craton in Texas and northern Chihuahua as revealed by Pb isotopes: Geological Society of America Bulletin, v. 105, p. 116–126.

John, B. E., 1988, Structural reconstruction and zonation of a tilted mid-crustal magma chamber: The felsic Chemehuevi Mountains plutonic suite: Geology, v. 16, p. 613–617.

John, D. A., 1995, Tilted middle Tertiary ash-flow calderas and subjacent granitic plutons, southern Stillwater Range, Nevada: Cross sections of an Oligocene igneous center: Geological Society of America Bulletin, v. 107, p. 180–200.

Johnson, A. M., and Pollard, D. D., 1973, Mechanics of growth of some laccolithic intrusions in the Henry Mountains, Utah, I. Field observations, Gilbert's model, physical properties, and flow of the magma: Tectonophysics, v. 18, p. 261–309.

Komuro, H., 1987, Experiments on cauldron formation: A polygonal cauldron and ring fractures: Journal of Volcanology and Geothermal Research, v. 31, p. 139–149.

Kunk, M. J., Sutter, J. F., and Naeser, C. W., 1985, High-precision $^{40}Ar/^{39}Ar$ ages of sanidine, biotite, hornblende, and plagioclase from the Fish Canyon Tuff, San Juan volcanic field, south-central Colorado: Geological Society of America Abstracts with Programs, v. 17, p. 636.

Lambert, J. R., Dokka, R. K., and Baksi, A. K., 1987, Lead Mountain caldera complex: Earliest Tertiary magmatism in the central Mojave Desert, California: Geological Society of America Abstracts with Programs, v. 19, no. 7, p. 738.

Lipman, P. W., 1976, Caldera-collapse breccias in the western San Juan Mountains, Colorado: Geological Society of America Bulletin, v. 87, p. 1397–1410.

Lipman, P. W., 1984, The roots of ash flow calderas in western North America: Windows into the tops of granitic batholiths: Journal of Geophysical Research, v. 89, p. 8801–8841.
Lipman, P. W., Self, S., and Heiken, G., 1984, Introduction to calderas special issue: Journal of Geophysical Research, v. 89, p. 8219–8221.
Lipman, P. W., Dungan, M. A., Brown, L. L., and Deino, A., 1996, Recurrent eruption and subsidence at the Platoro caldera complex, southeastern San Juan volcanic field, Colorado: New tales from old tuffs: Geological Society of America Bulletin, v. 108, p. 1039–1055.
Lonsdale, J. T., 1940, Igneous rocks of the Terlingua-Solitario region, Texas: Geological Society of America Bulletin, v. 51, p. 1539–1626.
Lynn, H. B., Hale, L. D., and Thompson, G. A., 1981, Seismic reflections from the basal contacts of batholiths: Journal of Geophysical Research, v. 86, p. 10633–10638.
Lyons, J. B., Campbell, J. G., and Erikson, J. P., 1996, Gravity signatures and geometric configurations of some Oliverian plutons: Their relation to Acadian structures: Geological Society of America Bulletin, v. 108, p. 872–882.
Mahon, K. I., Harrison, T. M., and Drew, D. A., 1988, Ascent of a granitoid diapir in a temperature varying medium: Journal of Geophysical Research, v. 93, p. 1174–1188.
Marsh, B. D., 1984, On the mechanics of caldera resurgence: Journal of Geophysical Research, v. 89, p. 8245–8251.
Marsh, B. D., 1989, Magma chambers: Annual Review of Earth and Planetary Sciences, v. 17, p. 439–474.
Marti, J., Ablay, G. J., Redshaw, L. T., and Sparks, R. S. J., 1994, Experimental studies of collapse calderas: London, Journal of the Geological Society, v. 151, p. 919–929.
Maxwell, R. A., Lonsdale, J. T., Hazzard, R. T., and Wilson, J. A., 1967, Geology of Big Bend National Park, Brewster County, Texas: University of Texas at Austin, Bureau of Economic Geology Publication 6711, 320 p.
McConnell, V. S., Shearer, C. K., Eichelberger, J. C., Keskinen, M. J., Layer, P. W., and Papike, J. J., 1995, Rhyolite intrusions in the intracaldera Bishop Tuff, Long Valley caldera, California: Journal of Volcanology and Geothermal Research, v. 67, p. 41–60.
McIntosh, W. C., Sutter, J. F., Chapin, C. E., and Kedzie, L. L., 1990, High-precision $^{40}Ar/^{39}Ar$ sanidine geochronology of ignimbrites in the Mogollon-Datil volcanic field, southwestern New Mexico: Bulletin of Volcanology, v. 52, p. 584–601.
Morgan, S. S., and Law, R. D., 1996, Concordant aureoles and multiple pulses of metamorphism: Reducing the pluton emplacement problem by multiple injections of magma: Geological Society of America Abstracts with Programs, v. 28, no. 7, p. A-436.
Mudge, M. R., 1968, Depth control of some concordant intrusions: Geological Society of America Bulletin, v. 79, p. 315–332.
Nabelek, P. I., Russ-Nabelek, D., and Denison, J. R., 1992, The generation and crystallization conditions of the Proterozoic Harney Peak Leucogranite, Black Hills, South Dakota, U.S.A.: Petrologic and geochemical constraints: Contributions to Mineralogy and Petrology, v. 110, p. 173–191.
Paterson, S. R., and Fowler, T. K., Jr., 1993, Extensional pluton-emplacement models: Do they work for large plutonic complexes?: Geology, v. 21, p. 781–784.
Paterson, S. R., and Fowler, T. K., Jr., 1995, Bursting the bubble of ballooning plutons: A return to nested diapirs emplaced by multiple processes: Geological Society of America Bulletin, v. 107, p. 1356–1380.
Petford, N., 1996, Dykes or diapirs?, *in* Brown, M., Candela, P. A., Peck, D. L., Stephens, W. E., Walker, R. J., and Zen, E-an, eds., The third Hutton symposium on the origin of granites and related rocks: Geological Society of America Special Paper 315, p. 105–114.
Petford, N., Kerr, R. C., and Lister, J. R., 1993, Dike transport of granitoid magmas: Geology, v. 21, p. 845–848.
Pitcher, W. S., 1979, The nature, ascent and emplacement of granitic magmas: Journal of the Geological Society of London, v. 136, p. 627–662.
Pollard, D. D., and Johnson, A. M., 1973, Mechanics of growth of some laccolithic intrusions in the Henry Mountains, Utah, II. Bending and failure of overburden layers and sill formation: Tectonophysics, v. 18, p. 311–354.
Powers, S., 1921, Solitario uplift, Presidio-Brewster Counties, Texas, *in* Morris, E. M., and Pasteris, J. D., eds., Mantle metasomatism and alkaline magmatism: Geological Society of America Bulletin, v. 32, p. 417–428.
Price, J. G., Henry, C. D., Barker, D. S., and Parker, D. F., 1987, Alkalic rocks of contrasting tectonic settings in Trans-Pecos Texas: Geological Society of America Special Paper 215, p. 335–346.
Redden, J. A., Norton, J. J., and McLaughlin, R. J., 1985, Geology of the Harney Peak Granite, Black Hills, South Dakota, *in* Rich, R. J., ed., Geology of the Black Hills, South Dakota and Wyoming: Alexandria, Virginia, American Geological Institute, p. 225–240.
Roman-Berdiel, T., Gapais, D., and Brun, J. P., 1995, Analogue models of laccolith formation: Journal of Structural Geology, v. 17, p. 1337–1346.
Scaillet, B., Pecher, A., Rochette, P., and Champenois, M., 1995, The Gangotri granite (Barhwal Himalaya): Laccolithic emplacement in an extending collisional belt: Journal of Geophysical Research, v. 100, p. 585–607.
Scandone, R., 1990, Chaotic collapse of calderas: Journal of Volcanology and Geothermal Research, v. 42, p. 285–302.
Self, S., Goff, F., Gardner, J. N., Wright, J. V., and Kite, W. M., 1986, Explosive rhyolitic volcanism in the Jemez Mountains: Vent locations, caldera development, and relation to regional structure: Journal of Geophysical Research, v. 91, p. 1779–1798.
Sides, J. R., 1980, Emplacement of the Butler Hill Granite, a shallow pluton within the St. Francois Mountains batholith, southeastern Missouri: Geological Society of America Bulletin, v. 91, p. 535–540.
Sides, J. R., Bickford, M. E., Shuster, R. D., and Nusbaum, R. L., 1981, Calderas in the Precambrian terrane of the St. Francois Mountains, southeastern Missouri: Journal of Geophysical Research, v. 86, p. 10349–10364.
Simony, P., and Halwas, D., 1993, Emplacement of a granitic sheet by multiple intrusion: Geological Society of America Abstracts with Programs, v. 25, no. 6, p. A-304.
Smith, R. L., 1979, Ash-flow magmatism, *in* Chapin, C. E., and Elston, W. E., eds., Ash-flow tuffs:: Geological Society of America Special Paper 180, p. 5–27.
Smith, R. L., and Bailey, R. A., 1968, Resurgent cauldrons, *in* Coats, R. R., Hay, R. L., and Anderson, C. A., eds., Studies in volcanology: Geological Society of America Memoir 116, p. 613–662.
Spell, T. L., Kyle, P. R., Thirlwall, M. F., and Campbell, A. R., 1993, Isotopic and geochemical constraints on the origin and evolution of postcollapse rhyolites in the Valles caldera, New Mexico: Journal of Geophysical Research, v. 98, p. 19723–19739.
Stachel, T., Lorenz, V., and Stanistreet, I. G., 1994, Gross Brukkaros (Namibia): An enigmatic crater-fill reinterpreted as due to Cretaceous caldera evolution: Bulletin of Volcanology, v. 56, p. 386–397.
Sweeney, J. F., 1976, Subsurface distribution of granitic rocks, south-central Maine: Geological Society of America Bulletin, v. 87, p. 241–249.
Vejmelek, L., and Smithson, S. B., 1995, Seismic reflection profiling in the Boulder batholith, Montana: Geology, v. 23, p. 811–814.
Vigneresse, J. L., 1995, Crustal regime of deformation and ascent of granitic magma: Tectonophysics, v. 249, p. 187–202.
Walker, G. P. L., 1972, Crystal concentration in ignimbrites: Contributions to Mineralogy and Petrology, v. 36, p. 135–146.
Walker, G. P. L., 1984, Downsag calderas, ring faults, caldera sizes, and incremental caldera growth: Journal of Geophysical Research, v. 89, p. 8407–8416.
Wells, R. E., 1979, Drake Peak: A structurally complex rhyolite center in southeastern Oregon: U.S. Geological Survey Professional Paper 1124-E, p. E1–E15.
Wilson, L., Sparks, R. S. J., and Walker, G. P. L., 1980, Explosive volcanic eruptions, IV. The control of magma properties and conduit geometry on eruption column behaviour: Geophysical Journal, Royal Astronomical Society, v. 63, p. 117–148.
Wood, C. A., 1984, Calderas: A planetary perspective: Journal of Geophysical Research, v. 89, p. 8391–8406.

MANUSCRIPT RECEIVED BY THE SOCIETY APRIL 19, 1996
REVISED MANUSCRIPT RECEIVED NOVEMBER 17, 1996
MANUSCRIPT ACCEPTED DECEMBER 11, 1996

Printed in U.S.A.